

The Benchmark Greenium*

Stefania D’Amico[†], Johannes Klausmann[‡] and N. Aaron Pancost[§]

This version: March 14, 2024

Abstract

Exploiting the unique “twin” structure of German government green and conventional securities, we use a dynamic term structure model to estimate a frictionless sovereign risk-free greenium, distinct from the yield spread between the green security and its conventional twin (the green spread). The model purifies the green spread from confounding and idiosyncratic factors unrelated to environmental concerns. While the model-implied greenium exhibits a significant relation with proxies of shocks to climate concerns—and the green spread does not—the green spread correlates with stock market prices and measures of flight-to-quality. We also estimate the greenium term structure and expected green returns.

Keywords: ESG, green bonds, dynamic no-arbitrage models
JEL Classifications: G12, Q51

*We thank Michael Bauer, Valère Fourel, Anh Le (discussant), Sara Mouabbi, Daniel Neuhann, Trang Nguyen (discussant), Lubos Pastor, Anna Pavlova, Rich Rosen, Guillaume Roussellet, Jakob Shida, Laura Starks, Luke Taylor, David Zerbib (discussant), and seminar participants at the McCombs Finance Brownbag, the 2022 Paris Asset Pricing Breakfast, the 11th Annual Term Structure Workshop at the Bundesbank, McGill University (Desautels), the Chicago Fed, Colorado State University, the 9th International Symposium on Environment and Energy Finance Issues (ISEFI), the 8th Bank of Canada / Federal Reserve Bank of San Francisco Conference on Fixed Income Markets, and the 98th Annual International Banking Economics and Finance Association (IBEFA) Summer Meeting for helpful comments and conversations. All remaining errors are our own. We thank Robert Bernhardt and Brian Wickman for outstanding research assistance. The views expressed here do not reflect official positions of the Federal Reserve.

[†]Federal Reserve Bank of Chicago. Contact: stefania.damico@chi.frb.org

[‡]University of Virginia, Darden School of Business. Contact: KlausmannJ@darden.virginia.edu

[§]University of Texas at Austin McCombs School of Business. Contact: aaron.pancost@mcombs.utexas.edu

1 Introduction

Investments of at least \$5 trillion per year are needed by 2030 to meet climate goals compatible with the Paris Climate Agreement.¹ Mobilizing public and private financial resources is key to generating the trillions of dollars needed for the rapid transition required. One possible strategy to raise public finances is to issue sovereign green bonds—government-guaranteed bonds whose proceeds are exclusively used to fund environmentally-sustainable (green) projects—and, indeed, many countries have already done so.

In this paper, we study the *benchmark greenium*, the frictionless premium of sovereign risk-free green securities relative to otherwise identical non-green securities. Identifying this type of greenium is important for two reasons. First, since sovereign green bonds are not project-specific, in the absence of market frictions, our greenium will capture the shadow value of wide environmental concerns. Second, because bids in the primary auction market depend largely on resale prices in the secondary market, the benchmark greenium provides a signal about future savings from the issuance of green securities.

In order to estimate the shadow value of environmental concerns, it is necessary to purge any measured greenium of market frictions related to the specific characteristics of the green security relative to the non-green security. Such relative frictions (e.g., liquidity and safety premiums of the more established non-green securities) can be large enough to offset this shadow value, and thus the subsidy investors are willing to provide the government to finance green projects, limiting the information content of the measured greenium. A greenium purged of market frictions, being a better measure of the subsidy, provides a more informative signal about potential interest cost savings.

Since the benchmark greenium is not directly observable from security prices, our estimation begins by exploiting a natural experiment: the novel “twin” structure of German federal green securities. Each of these securities is issued to finance only green projects and

¹Based on World Resource Institute estimates reported in 2021. Alternative estimates are even larger: 2018 OECD estimates are of \$6.9tr per year and UN IPCC \$2.4tr per year in the energy sector alone.

is paired with a conventional “twin:” a security with identical cash-flows and maturity, but not tied to green projects. In principle, the yield spread between the green and conventional twins—the *green spread*—ought to be a model-free measure of the greenium, as the conventional yield should “control for” all factors affecting German sovereign yields, except for those related to environmental concerns.

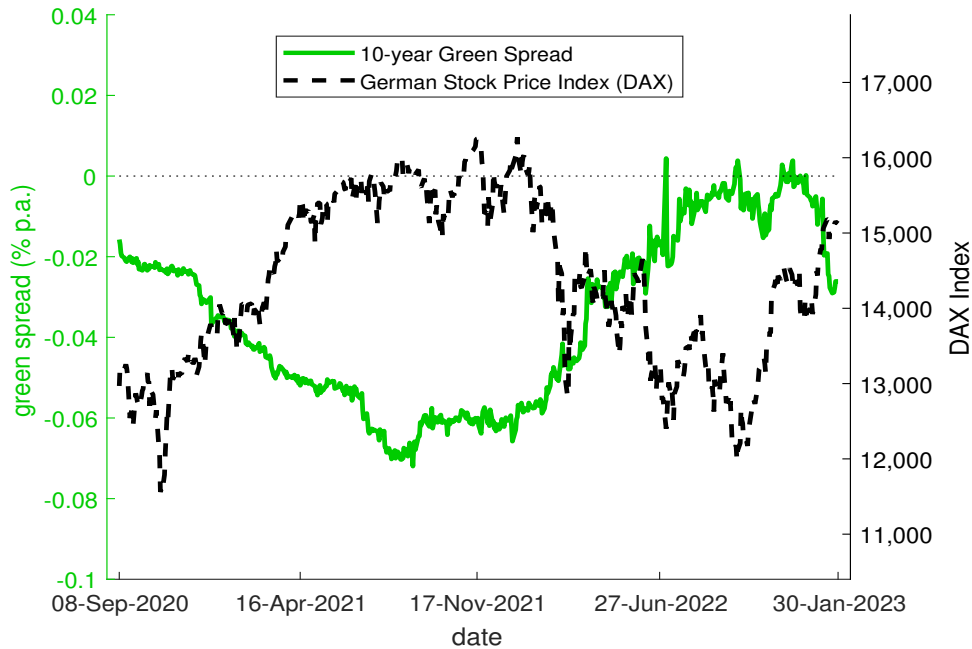


Figure 1. Relation between the Green Spread and Stock Prices

The green line depicts the yield spread between the green security maturing on August 15, 2030 and its conventional twin issued by the German government in September 2020, with values on the left axis, and the black line depicts the German Stock Price Index (DAX), with values on the right axis.

However, Figure 1 casts doubt on the reliability of the green spread as a direct measure of the premium stemming only from environmental concerns. The figure shows that, by the end of 2022, the green spread has reverted to nearly zero. Should one conclude that investors are no longer concerned about the environment, and therefore not willing to subsidize the green transition? Not necessarily. Indeed, Figure 1 reveals that the green spread is inversely related to the German stock market index, suggesting that risk factors unrelated to investors’ environmental preferences can drive a wedge between the observable green spread and the

benchmark greenium.

Importantly, from the behavior of the green spread alone, one cannot tell whether the green or conventional bond is the source of the market friction generating the greenium mispricing. For instance, demand/supply imbalances between the two securities can originate from flight-to-quality to the conventional bond or the smaller issuance size of the green bond. Further, each green spread relies on a single pair of twins, ignoring systematic information in the prices of other traded pairs of twins, as well as the full cross-section of conventional bonds.² This information is crucial to separate the benchmark greenium from other systematic risk factors.

We introduce a security-level no-arbitrage dynamic term-structure model (DTSM) that jointly prices all outstanding German federal green and conventional securities, allowing us to estimate a time-varying greenium effectively purged of factors unrelated to environmental concerns. This is because we price all bonds using a set of common conventional factors and an additional “green” factor that affects only green bonds.³ By extracting information common to all green and conventional securities, the estimated daily conventional and green yield curves capture only systematic financial/economic factors, including those related to environmental concerns. The difference between these two yield curves provides a benchmark greenium at every maturity—a frictionless greenium term structure.

We have three main findings. First, the model-implied benchmark greenium differs substantially from the observed green spread: it tends to be significantly larger; at times it widens while the green spread narrows; and its term structure is mostly flat, rather than downward-sloping. Second, proxies of confounding and idiosyncratic risk factors, such as stock market prices, measures of flight-to-quality, and liquidity, do not affect the model-implied greenium, but do correlate with the green spread. Conversely, the benchmark gree-

²At the time of this writing, there are five green spreads available, and as we will show later, each of them conveys different information. Figure 1 plots the green spread with the longest time series.

³The green spread cannot be “arbitraged away,” because the green security is subject to shocks to green preferences, that is, the green factor is a stochastic risk factor. Hence a simple strategy long the conventional and short the green is not riskless.

nium correlates with shocks to environmental concerns, such as the economic damages from environmental disasters—which in our sample are mainly driven by the devastating German floods in the summer of 2021. Interestingly, once we control for confounding and idiosyncratic risk factors, the green spread does not correlate significantly with shocks to environmental concerns.

Third, the difference between the expected return on green and conventional bonds, the expected green excess return, varies with the investment horizon and investors' information set: it is positive at issuance and turns negative after the German floods. In line with Pastor, Stambaugh and Taylor (2021), as investors become more concerned about the environment, they are willing to accept lower expected returns to hold green assets, consistent with a widening benchmark greenium. Furthermore, as suggested by Pastor, Stambaugh and Taylor (2022), the expected and realized green excess returns diverge when there is an unanticipated change in climate concerns; but, they diverge also when there are surprises unrelated to environmental preferences, such as the start of the Ukrainian war that triggered a flight to quality to German conventional securities. This finding is consistent with a green spread that, differently from the benchmark greenium, is affected by confounding and idiosyncratic risk factors. In our sample, while shocks to climate concerns trigger unexpected inflows into green securities, causing them to perform better than expected, shocks to risk attitudes trigger unexpected inflows into their conventional twins, causing green securities to perform worse than expected.

Our findings are important not only because they indicate that green spreads should not be taken at their face value to price environmental concerns, but also due to their policy implications. First, the fact that the benchmark greenium is not reverting to zero over time signals that green security issuance can provide interest cost savings to governments.⁴ However, to access these savings, government finance agencies need to minimize market frictions. Second, a persistent benchmark greenium justifies the inclusion of green assets by

⁴Semmler et al. (2021) show that green bonds can be useful financial instruments in fiscal policies for a transition to a low-carbon economy.

central banks in the conduct of conventional and unconventional monetary policy, since it indicates investors’ clear preference for green investments, and eligibility for central bank operations reduces liquidity risks and other frictions affecting these assets, especially in periods of crisis.⁵ Third, a risk-free benchmark greenium will allow for more efficient pricing of private green securities, strengthening the market for green investments.⁶

Our work has been informed by different strands of the literature. First, Pastor, Stambaugh and Taylor (2021) and Zerbib (2022) show mechanisms through which environmental preferences can generate a “taste” premium in green stocks, which motivate our search for the greenium in green government bonds. Second, Pastor, Stambaugh and Taylor (2022), despite being focused on the US stock market, are the first to use German twin bonds to illustrate the widening of the green spread during periods of heightened climate concerns.

Third, our paper is closely related to several empirical studies assessing the value of green bonds relative to otherwise similar non-green bonds. They show that greenium estimates in municipal and corporate bond markets vary greatly: from zero (Larcker and Watts, 2020), to relatively small (-8 bps in Caramichael and Rapp 2022, -6 bps in Baker et al. 2018, and -2 bps in Zerbib 2019), to sizable (-63 bps in Colombage and Nanayakkara 2020).⁷ Further, Karpf and Mandel (2018), Flammer (2021), Kapraun et al. (2021), Berg et al. (2021), and Berg, Kölbel and Rigobon (2022) highlight factors different from environmental preferences that affect greenium estimates, such as issuance size, creditworthiness and credibility of the issuer, as well as noise in ESG ratings. Differently from all these studies, we focus on German sovereign bonds and use a DTSM, hence we can obtain risk-free time-varying estimates of the greenium and its term structure. Importantly, this allows us to analyze the drivers of the benchmark greenium’s fluctuations and to study ex-ante expected green returns, which makes us well equipped to test the theory of Pastor, Stambaugh and Taylor (2021) for

⁵Papoutsis, Piazzesi and Schneider (2021), Riedler and Koziol (2021), and Hansen (2022) analyze the tilting of central banks’ portfolio allocations toward green and away from brown assets in the conduct of unconventional monetary policy.

⁶See for example the GFA’s 2020 [Green Bond Framework](#).

⁷The size of the greenium, by increasing the relative cost of capital of brown firms, also speaks to the debate over divestment vs. engagement (Edmans, Levit and Schneemeier, 2022; Hartzmark and Shue, 2023).

government green bonds.

More broadly, our research also relates to the literature investigating the pricing of climate change risks in financial markets.⁸ However, in line with a key distinction in Laura Starks’ AFA 2023 presidential address (Starks, 2023), we focus on the pricing of ESG investors’ *values*, rather than the financial *value* of ESG investing. There is ample evidence that socially responsible investors are willing to pay a premium to access securities that are aligned with their value system.⁹ Like Zerbib (2019), our premise is that the greenium, being related to environmental preferences, should not be driven by pecuniary motives, such as hedging financial losses due to climate change.¹⁰ The benchmark greenium that we isolate is a dividend that investors are willing to forgo to fund green projects, providing a subsidy to the government.

2 Green Spreads: Benefits and Limitations

Germany issued its first green sovereign bond in September 2020, and since then its green securities have accounted for about 3 percent of the total amount outstanding of German government securities. Overall, Germany is the second-largest issuer of sovereign green bonds in the world, and the first to issue green bonds alongside conventional twins. See Appendix A for background information on the green bond market.

Every green bond issued by the German Finance Agency (GFA) is paired with a conventional “twin” bond which has the exact same maturity date and coupon structure. Table 1 lists the salient characteristics of the five German green securities and their conventional

⁸See for example Bansal, Kiku and Ochoa (2016), Bernstein, Gustafson and Lewis (2019), Engle et al. (2020), Gibson, Krueger and Mitali (2020), Kling et al. (2020), Krueger, Sautner and Starks (2020), Painter (2020), Alekseev et al. (2021), Bauer and Rudebusch (2021), Giglio et al. (2021), Huynh and Xia (2021), Ilhan, Sautner and Vilkov (2021), Cevik and Jalles (2022), and Chikhani and Renne (2022). A more recent strand of the literature (e.g. Berrada et al. 2022, Kölbel and Lambillon 2022 & Loumioti and Serafeim 2022) prices so-called sustainability-linked bonds or loans.

⁹See for example Riedl and Smeets (2017), Hartzmark and Sussman (2019), Bauer, Ruof and Smeets (2021), Guenster et al. (2022), Bonnefon et al. (2022), and Heeb et al. (2023).

¹⁰See for example Bolton and Kacperczyk (2021), Pedersen, Fitzgibbons and Pomorski (2021), Stroebel and Wurgler (2021), and Sautner et al. (2023).

twins issued from September 2020 to September 2022.

ISIN	Issue Date	Maturity	Coupon	Amount (Bil \$)	Green
DE0001102507	2020-06-19	2030-08-15	0	35.2	0
DE0001030708	2020-09-09	2030-08-15	0	8.81	1
DE0001141828	2020-07-10	2025-10-10	0	27.5	0
DE0001030716	2020-11-06	2025-10-10	0	5.51	1
DE0001102481	2019-08-23	2050-08-15	0	33.6	0
DE0001030724	2021-05-18	2050-08-15	0	6.61	1
DE0001102564	2021-06-18	2031-08-15	0	32.5	0
DE0001030732	2021-09-10	2031-08-15	0	7.16	1
DE0001141869	2022-06-30	2027-10-15	1.3	29.3	0
DE0001030740	2022-09-07	2027-10-15	1.3	5.43	1

Table 1. German Twin Bonds

This table lists all German sovereign green bonds and their respective twins. The pairs exhibit matching maturity dates and coupon rates. The USD amount issued is the total amount outstanding. The last column indicates whether the bond is green (1) or conventional (0).

Indeed, as shown in the third and fourth columns, for each pair of twins, the maturity and coupons are identical, suggesting that the yield spread between the two twins (the green spread) could provide a model-free measure of the greenium. However, as shown in the second and fifth columns, the twins’ issue dates can be up to 21 months apart, implying that their ages differ, and the issuance amount is much smaller for green bonds, suggesting relative liquidity and scarcity differentials.¹¹ This indicates that green spreads may have limitations that impair the greenium measurement.

In the remainder of this section, we discuss in more detail the advantages and disadvantages of using the green spread as an estimate of the greenium. This is important as our goal is to develop a model that leverages the advantages of German green spreads, while reducing the impact of their limitations, allowing us to estimate a greenium that reflects environmental concerns more closely than the simple green spread.

¹¹Krishnamurthy (2002), Fontaine and Garcia (2012), and Pancost (2021) analyze the role of bond age in price anomalies related to their liquidity.

2.1 Benefits

German federal green bonds offer several advantages over other green securities when it comes to estimating the benchmark greenium. First, since German debt is risk-free, security cash-flows are known with certainty and therefore any price differential between green and brown securities must represent a difference in discount rates. In contrast, greenium estimates in virtually any other asset class (corporate bonds, municipal bonds, equities) potentially combine a difference in discount rates with a difference in cash-flows.

Second, the GFA is committed to ensuring that the green bond is at least as liquid as its conventional twin. Liquidity differences between bonds can be of first-order importance for understanding spreads (D’Amico, Kim and Wei, 2018), and the fact that green bond issuances are substantially smaller than their corresponding twins (Table 1), combined with the novelty of the instrument, may make green bonds less liquid. The GFA employs two tools, switch trades and green repos, to allay fears that the smaller green securities will trade at a discount with respect to the conventional bond in the secondary market. Switch trades provide investors with the option to convert a green bond into its conventional twin without penalty at any time. Green repos consist of GFA’s temporary purchases of a green bond if its price falls below the conventional twin’s price, providing the green security with an implicit pricing floor.¹²

Third, ISS ESG, one of the world’s leading independent rating agencies in the field of sustainable investments, awarded Germany a green rating of B and classified it as PRIME, on a rating scale from A+ (excellent) to D- (poor). According to ISS ESG, “as of August 21, 2020, this rating puts Germany in place 12 out of 124 countries rated by ISS ESG. This equates to a high relative performance, with a decile rank of 1.”

Fourth, the proceeds of German green bonds are more transparently allocated than other green securities, allaying concerns of “fungibility.” Deloitte conducts an external audit to

¹²For more detail see <https://www.deutsche-finanzagentur.de/en/institutional-investors/federal-securities/green-federal-securities/>

verify the actual allocation of issue proceeds to green expenditures. Afterwards, the federal government provides two reports to the public: an allocation report linking final green expenditures to last year’s green bond issuance, and one year later an impact report detailing the impact of green spending on the environment and climate.¹³

Finally, Germany’s green bond issuance costs are non-recurrent, making issuance less costly and time consuming than the issuance of green bonds by private corporations. Many elements of the certification process outlined above occur mainly at the country rather than the bond level. Furthermore, many of these costs are fixed, in the sense that they do not need to be borne again were the issue to be re-opened.

2.2 Limitations

Despite the advantages of the novel twin structure, there remain some conceptual and practical difficulties with using the green spread as a direct measure of the greenium.

First of all, no green spread provides a constant-maturity reading of the greenium. Second, each green spread, relying on a single pair of bonds, ignores information contained in the prices of the other pairs of twins and in the full term structure of German federal securities. Hence, any factors specific to the particular pair of twins—for instance, differences in the issuance size, dates, and method—will contaminate the green spread.¹⁴ We call these factors “idiosyncratic” factors. Third, the green spread can be affected by risk factors common to all pairs of twins but unrelated to environmental preferences. We call these factors “confounding” factors. Both idiosyncratic and confounding factors can cause temporary mispricing of the benchmark greenium.

Figure 2 plots the five green spreads (i.e., the sovereign yield spread between each of the five pairs of green and conventional twin bonds), and shows ample evidence of greenium mispricing. For instance, the first clear example of the importance of idiosyncratic factors

¹³For more detail see <https://www.deutsche-finanzagentur.de/en/institutional-investors/federal-securities/green-federal-securities/>

¹⁴By issuance method, we mean regular auction as opposed to syndication. Three of the five green bonds in our sample were issued via syndicate, whereas all five conventional twins were issued via regular auction.

is given by the difference between the dark blue and black lines. Both depict green spreads that had an original maturity of 10 years but have been issued one year apart. In principle, since the average shadow value of environmental concerns over the next 9 or 10 years should be nearly identical, if these two green spreads were capturing only this shadow value, they should be very close. But they are not.

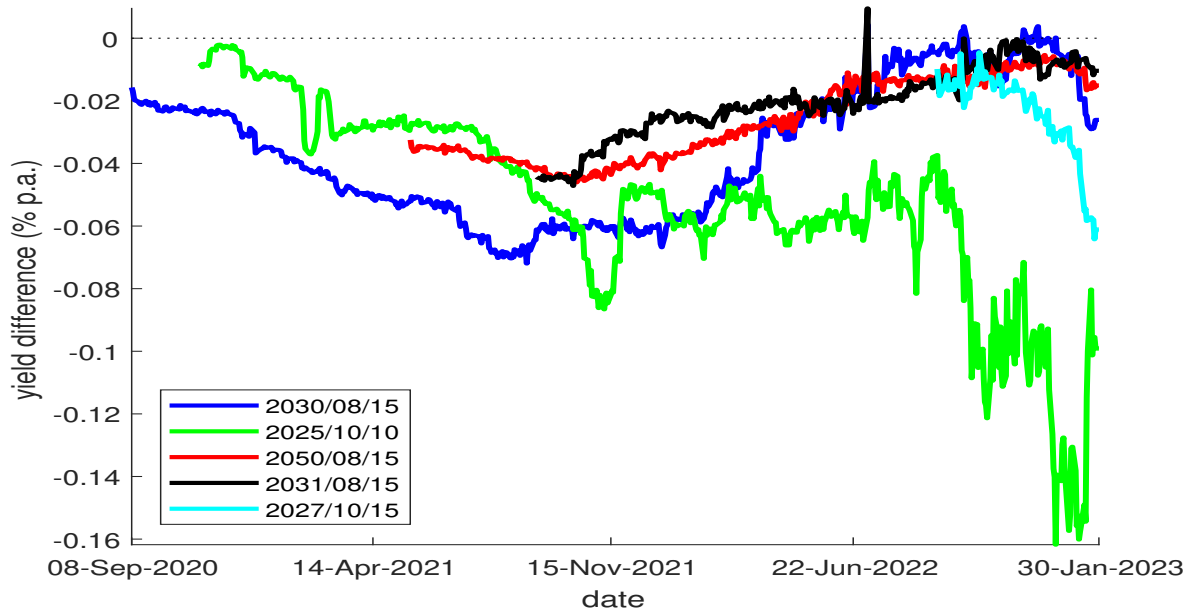


Figure 2. German Green Spreads

The figure plots the yield differences $Y_{i,t}^g - Y_{i,t}$ for five pairs of German sovereign bonds. Each pair has the same coupon structure and maturity date, but one of the bonds in each pair is a certified “green” bond, whose cash-flows are earmarked for sustainable investments.

The second example is provided by the unique behavior of the green spread expiring in 2025, shown in green. Only this spread widened to 16 basis points at the end of 2022, most likely as official and private investors aiming at reducing their portfolios’ carbon footprint loaded on the shortest maturity green bond. For instance, the European Central Bank (ECB) has increased the share of green bonds in its own funds portfolio, which mainly consists of euro area government bonds, up from 1% in 2019 to 13% in 2022.¹⁵ As soon as the GFA

¹⁵The ECB’s euro-denominated non-monetary policy portfolios include its own funds portfolio and its staff pension fund; and, in March 2023, the ECB has started disclosing the climate impact of its portfolio, see “Climate-related financial disclosures of the ECB’s non-monetary policy portfolios,” March 2023.

re-opened the green security at auction (thereby increasing its supply), the shortest maturity spread started reverting toward the other spreads, suggesting that this isolated fluctuation was unrelated to changes in environmental concerns.

Overall, any short-lived episode that causes demand/supply imbalances between green and conventional securities might affect the green spread but has nothing to do with environmental preferences. On the one hand, stronger demand at auctions for green bonds combined with their smaller issuance size can make these bonds scarcer than conventional bonds. On the other hand, the ECB's purchases of large amounts of conventional bonds, as well as the flight to quality to those bonds, may induce conventional bonds to be scarcer than green bonds. Further, also the green securities' implicit pricing floor (mentioned in Section 2.1) can contaminate green spreads. German green bonds contain an embedded put option as the GFA would not let their price fall below the price of their conventional twins. As shown in Figure 2, this option is usually out of the money and therefore has little value, but could have moved into the money toward the end of the sample as the price of green bonds briefly fell below that of conventional bonds, especially for the most recently issued green bonds. However, in our approach, the green yields are derived from a curve fitted to the entire universe of green and conventional securities, which makes them less susceptible to the effect of the implicit pricing floor compared to a single green spread.

More formally, let Y_t^g be the yield on a hypothetical riskless constant-maturity green bond at time t , and let Y_t be the yield on an otherwise-identical conventional bond.¹⁶ Let i denote a particular twin pair, so that $Y_{i,t}^g$ is the yield on the green bond and $Y_{i,t}$ the yield

¹⁶Andreasen, Christensen and Rudebusch (2019) and Pancost (2021) note that yields on constant-maturity bonds are not observable in practice, and must be inferred from the prices of actual bonds whose maturity declines over time.

on its conventional twin. Then the green spread for pair i can be written as

$$\begin{aligned}
Y_{i,t}^g - Y_{i,t} &= (Y_t^g + \tilde{\varepsilon}_{i,t}^g) - (Y_t + \tilde{\varepsilon}_{i,t}) \\
&= \left[(Y_t^{*g} + \tilde{\varepsilon}_t^g) + \tilde{\varepsilon}_{i,t}^g \right] - \left[(Y_t^* + \tilde{\varepsilon}_t) + \tilde{\varepsilon}_{i,t} \right] \\
&= \underbrace{Y_t^{*g} - Y_t^*}_{\text{benchmark greenium}} + \underbrace{\tilde{\varepsilon}_t^g - \tilde{\varepsilon}_t}_{\text{premium on confounding factors}} + \underbrace{\tilde{\varepsilon}_{i,t}^g - \tilde{\varepsilon}_{i,t}}_{\text{premium on idiosyncratic factors}}
\end{aligned} \tag{1}$$

where $\tilde{\varepsilon}_{i,t}^g$ and $\tilde{\varepsilon}_{i,t}$ are the idiosyncratic factors affecting only the two bonds in the pair i , and ε_t^g and ε_t are the additional confounding factors common to all pairs of twins. In equation (1), $Y_t^g - Y_t$ would be the green spread purged of the bond-specific idiosyncratic factors; but it still differs from the benchmark greenium $Y_t^{*g} - Y_t^*$ because of the confounding factors.

To purge our estimates of the greenium from the relative mispricing induced by idiosyncratic and confounding factors, in the next section we introduce a DTSM framework that jointly prices German nominal green and conventional securities. On each day, the model produces separate conventional and green yield curves. Because each curve is constructed using all available bond prices, the greenium at any given maturity is a function of systematic factors and hence free of any idiosyncratic factors. In addition, since the DTSM prices bonds only according to their “cash flows”—including non-pecuniary green benefits—our greenium is free of confounding factors as well.¹⁷

3 The Model

In this section, we present our model and the estimation details. Importantly, the model described in this section is not merely a yield-curve-fitting exercise; it will price conventional and green securities dynamically according to a time-series model of both conventional and green discount rates. In particular, investors will price both types of bonds, at all maturities,

¹⁷Unfortunately, our setup does not allow us to separate the idiosyncratic factors $\tilde{\varepsilon}_{i,t}^g - \tilde{\varepsilon}_{i,t}$ from the confounding factors $\tilde{\varepsilon}_t^g - \tilde{\varepsilon}_t$ in equation (1), though this would be an interesting question for future research. However, we do identify the combination of these factors as residuals from the model estimation. In addition, these residuals are persistent as estimated in Appendix C.2.

on a given date by forecasting the time path of both green and conventional discount rates into the future. Relative to the conventional discount rate, the green discount rate is driven by an extra pricing factor, that is, the green factor, which is identified by price differences between green and conventional bonds in the cross-section. And importantly, the model considers all conventional bond prices when forming the conventional yield curve, allowing it to generate a relative “mispricing” of the conventional twins. Hence, in purifying the green spread from the relative mispricing of green and conventional securities, it is not just the mispricing of green bonds that matters, but also the mispricing of conventional twin bonds.

3.1 Model

We assume that the prices of German federal securities depend on a $k \times 1$ vector X_t that consists of latent factors, which evolve according to an Ornstein-Uhlenbeck process:

$$dX_t = \left[-\mu_x - \phi_x X_t \right] dt + \Sigma_x dW_t^x, \quad (2)$$

where W_t^x is a standard Brownian motion, and μ_x , ϕ_x , and Σ_x are estimated parameters that govern the time-series behavior of bond prices. Specifically, μ_x affects the mean value of the factors, ϕ_x their evolution as a function of past factors, and Σ_x their variance.

In order to price green bonds, we assume that ESG investors derive a flow of utility from investing in green bonds, and that this utility flow varies over time. Formally, investors receive a non-pecuniary utility flow of $G_t dt$, per unit of face value, where G_t is an additional pricing factor that only affects the prices of green bonds. The assumption of proportionality to face value seems natural in the ESG context, where the increase in utility investors derive from ESG investing is proportional to the amount invested, and not the current price of the

bond.¹⁸ We assume that G_t also follows an Ornstein-Uhlenbeck process

$$dG_t = [-\mu_g - \phi_g G_t] dt + \Sigma_g dW_t^g, \quad (3)$$

where W_t^g is a Brownian motion uncorrelated with W_t^x .

The stochastic discount factor (SDF) is of the linearity-generating (LG) form first derived by Gabaix (2007, 2008); it is given by

$$\frac{dM_t}{M_t} = -\left[\delta_0 + \delta_1' X_t\right] dt - \left[\sigma(X_t, G_t) - \begin{pmatrix} \Sigma_x^{-1} X_t \\ \Sigma_g^{-1} G_t \end{pmatrix} X_t' \delta_1\right] \cdot \begin{pmatrix} dW_t^x \\ dW_t^g \end{pmatrix} \quad (4)$$

where

$$\sigma(X_t, G_t) \equiv \begin{bmatrix} \lambda_0^x + \lambda_1^x X_t \\ \lambda_0^g + \lambda_1^g G_t \end{bmatrix}. \quad (5)$$

In order to price conventional bonds on a long sample that predates the introduction of green bonds, we make two implicit assumptions in equations (3–5). First, we assume that G_t does not affect the drift of the SDF in equation (4); thus, the short rate of interest depends only on the conventional factors X_t and is independent of G_t . This is not unreasonable considering that most central banks do not account for green factors in determining the stance of monetary policy. Second, because G_t does not appear in equation (2) at all, G_t does not contain any information useful for *forecasting* X_t —and with it, the short rate. Both assumptions allow us to estimate the time-series parameters of the conventional and green bonds separately.

Furthermore, in equation (5) we assume that the time-varying prices of risk $\sigma(X_t, G_t)$ are “block diagonal” in the sense that the first k elements depend only on X_t , while the

¹⁸In contrast, Duffie (1996) and D’Amico and Pancost (2021) show that the “dividend” arising from special repo spreads is proportional to the bond’s current price.

last element depends only on G_t . In other words, the price of G_t risk varies over time only with G_t ; changes in the conventional yield curve—represented by changes in the first k factors—have no effect on the price of G_t risk conditional on the value of G_t . The converse is also true; the prices of level, slope, and curvature risk can each vary with level, slope, and curvature, but are unaffected by G_t . These assumptions drastically reduce the number of “green” parameters to estimate, which is particularly important given the short sample for which we observe green bonds.

Although equations (3–5) imply that G_t and its prices of risk are conditionally independent of X_t , the model will still allow us to purge the green spreads in equation (1) of most idiosyncratic and confounding factors to recover the greenium. The reason is that the model-implied prices of a green bond will still depend on the conventional factors X_t , which will be estimated using the full cross-section of German conventional bonds (and not just the green bond’s twin).

Before deriving the no-arbitrage pricing condition, we comment briefly on why the assumption of no-arbitrage is valid in this setting. A non-zero green spread seems to violate the law of one price. Since both bonds pay the same (pecuniary) cash flows, an investor who does not value the green dividend ought to be able to short the expensive green bond, invest in the cheap conventional bond, and make money today while incurring no liabilities in the future. The key assumption behind this trade is that it is held to maturity, and there is no funding cost.

Time variation in the funding cost induces riskiness in the long-short strategy (D’Amico and Pancost, 2021). Moreover, any unwinding of the position before maturity involves risk: the green bond faces risk from the time-varying G_t dividend, which is stochastic. Thus, any long-short position that will be unwound before maturity involves two assets with merely *similar*, though not identical, cash-flows; in which case heterogeneity in green preferences, including some investors who do not value greenness at all, poses no issue for absence of arbitrage (Pastor, Stambaugh and Taylor, 2021).

The no-arbitrage pricing condition for a green zero-coupon bond is

$$0 = E_t \left\{ d(P_t^g(\tau) M_t) + M_t G_t dt \right\}, \quad (6)$$

which, along with the $X_t' \delta_1$ term in equation (4), ensures that prices of both green and conventional zero-coupon bonds are affine in the state, as the following proposition shows:

Proposition 1. *When the state evolves according to equations (2) and (3) and the SDF is given by equation (4), then the price of a conventional security that pays \$1 in τ periods when the factors are X_t is given by*

$$P_t(\tau) = A(\tau) + B(\tau)' X_t, \quad (7)$$

where the functions $A(\tau)$ and $B(\tau)$ are given by

$$\begin{pmatrix} A(\tau) \\ B(\tau) \end{pmatrix} = \exp \left\{ - \begin{bmatrix} \delta_0 & \mu_x^{*'} \\ \delta_1 & \phi_x^{*'} + \delta_0 I \end{bmatrix} \tau \right\} \begin{pmatrix} 1 \\ \vec{0} \end{pmatrix}, \quad (8)$$

$\exp \{ \cdot \}$ denotes matrix (not element-wise) exponentiation, and

$$\mu_x^* \equiv \mu_x - \Sigma_x \lambda_0^x \quad (9)$$

$$\phi_x^* \equiv \phi_x - \Sigma_x \lambda_1^x.$$

On the other hand, the price of a green security that pays a stream of dividends $G_t dt$ and also pays \$1 in τ periods when the factors are X_t is given by

$$P_t^g(\tau) = A^g(\tau) + B^g(\tau)' X_t + C^g(\tau) G_t, \quad (10)$$

where the functions $A^g(\tau)$, $B^g(\tau)$, and $C^g(\tau)$ are given by

$$\begin{pmatrix} 1 \\ A^g(\tau) \\ B^g(\tau) \\ C^g(\tau) \end{pmatrix} = \exp \left\{ - \begin{bmatrix} 0 & 0 & \vec{0} & 0 \\ \mu_g^* & \delta_0 & \mu_x^{*'} & \mu_g^* \\ \vec{0} & \delta_1 & \phi_x^{*'} + \delta_0 I & \vec{0} \\ \phi_g^* + \delta_0 & 0 & \vec{0} & \phi_g^* + \delta_0 \end{bmatrix} \tau \right\} \begin{pmatrix} 1 \\ 1 \\ \vec{0} \\ 0 \end{pmatrix}, \quad (11)$$

$\exp \{ \cdot \}$ denotes matrix (not element-wise) exponentiation, μ_x^* and ϕ_x^* are defined in equation (9), and

$$\begin{aligned} \mu_g^* &\equiv \mu_g - \Sigma_g \lambda_0^g \\ \phi_g^* &\equiv \phi_g - \Sigma_g \lambda_1^g \end{aligned} \quad (12)$$

Proof. See Appendix B.

3.2 Estimation Details

The linear pricing of Proposition 1 is convenient for pricing coupon bonds, which are portfolios of the zero-coupon bonds priced by equations (7) and (10). In fact, the price of a conventional bond i at time t is given by

$$P_{it} = \sum_{j=1}^{n_{it}} c_{ijt} \left[A(\tau_{ijt}) + B(\tau_{ijt})' \right] \begin{pmatrix} 1 \\ X_t \end{pmatrix}$$

where n_{it} is the number of total payments for bond i at time t , τ_{ijt} and c_{ijt} are the time and payment amounts of the j th payment. A similar equation holds for the price of a green

bond. Stacking all observable bonds at time t yields the measurement equation

$$\begin{pmatrix} P_t(\tau_{1,t}) \\ \dots \\ P_t(\tau_{n_t,t}) \\ P_t^g(\hat{\tau}_{1,t}) \\ P_t^g(\hat{\tau}_{2,t}) \\ \dots \end{pmatrix} = \underbrace{\begin{pmatrix} \vec{A}(\tau_{1,t}) & \vec{B}(\tau_{1,t})' & 0 \\ \dots & \dots & \dots \\ \vec{A}(\tau_{n_t,t}) & \vec{B}(\tau_{n_t,t})' & 0 \\ \vec{A}^g(\hat{\tau}_{1,t}) & \vec{B}^g(\hat{\tau}_{1,t})' & \vec{C}^g(\hat{\tau}_{1,t}) \\ \vec{A}^g(\hat{\tau}_{2,t}) & \vec{B}^g(\hat{\tau}_{2,t})' & \vec{C}^g(\hat{\tau}_{2,t}) \\ \dots & \dots & \dots \end{pmatrix}}_{Z(\tau_t, \theta^*)} \begin{pmatrix} 1 \\ X_t \\ G_t \end{pmatrix} + \vec{D}_t \odot \Sigma_t^M \varepsilon_t \quad (13)$$

where \vec{A} , \vec{B} , \vec{A}^g , \vec{B}^g , and \vec{C}^g are coupon-weighted sums of the relevant bond-price loadings, $\tau_{i,t}$ is the vector of payments and times to maturity of bond i 's payments at time t , and Σ_t^M is the variance of the measurement error at t . Pricing dozens of bonds with only a few factors requires the assumption that all prices are observed with some error. The vector \vec{D}_t contains the duration of each bond, which scales the measurement error in prices; doing so essentially weights each price observation by its inverse duration, akin to assuming that the measurement error is homoskedastic (to a first-order approximation) in yields rather than prices (Pancost, 2021). Omitting the \vec{D}_t term from equation (13) would result in a model fitting the long end of the yield curve much better than the short end.

Importantly, the elements of the vector ε_t are a combination of $\tilde{\varepsilon}_{i,t}$, $\tilde{\varepsilon}_{i,t}^g$, $\tilde{\varepsilon}_t$, and $\tilde{\varepsilon}_t^g$ from equation (1). Thus, we are not able to separately identify the idiosyncratic and confounding factors discussed above.

To estimate the model, in practice it is convenient to focus on the risk-neutral parameters $\theta^* \equiv \{\delta_0, \delta_1, \mu_x^*, \phi_x^*, \mu_g^*, \phi_g^*\}$, rather than the prices of risk $\{\lambda_0^x, \lambda_1^x, \lambda_0^g, \lambda_1^g\}$. The reason is that the matrix $Z(\tau_t, \theta^*)$ does not depend on the latent factors X_t and G_t —it depends only on the data (through τ_t) and θ^* . Independence from the factors means that $Z(\tau_t, \theta^*)$ can be constructed from the data and risk-neutral parameters alone, and then the factors can be estimated cross-section by cross-section using ordinary least squares and the sequential

regression filter of [Andreasen and Christensen \(2015\)](#). The sequential regression filter also allows us to estimate the time-series parameters in equations (2) and (3). This estimation approach—when combined with the LG model—is an order of magnitude faster than can be achieved using a standard exponential-affine model, where the time-series parameter Σ_x also appears in the measurement equation ([Pancost, 2021](#)).

We estimate the parameters pertaining to X_t on a long sample of conventional bond prices from October 27, 2008 to January 30, 2023. Because the model effectively de-couples the time-series and price-of-risk parameters for X_t and G_t , the time-series variation is relevant only to estimate expected returns, so that the benchmark greenium is identified solely from the cross-section of bond prices. [Appendix C](#) contains more details about our estimation procedure and estimated parameter values.

Because the factors X_t and G_t are unobservable, not all of the parameters in θ^* are identifiable. In particular, since any affine transformation of the X_t leads to the same fit to bond prices, only the eigenvalues of the matrix in equation (8) are identified. Thus, rather than estimating all $(k + 1)^2$ free parameters in this matrix, we normalize $\delta_1 = \begin{bmatrix} 1 & \vec{0} \end{bmatrix}'$ and $\phi_x^{*'} + \delta_0 = I$.¹⁹ In the end, only the $k + 1$ parameters in δ_0 and μ^* need to be estimated, when pricing conventional bonds. Pricing green bonds implies an additional two risk-neutral parameters, as can be seen in equation (11). These parameters are identified by the prices on green bonds.

4 Results

In this section, we discuss the results from estimating the model on conventional and green German sovereign securities. [Section 4.1](#) briefly describes the data, [Section 4.2](#) summarizes the model’s fit to the data, and [Section 4.3](#) focuses on our estimated greenium. Then, in [Section 5](#), we compare our estimated greenium to the green spread, and relate both to

¹⁹This normalization, though more complicated than (for example) $\mu^* = \vec{0}$ and a diagonal ϕ_x^* , does not restrict the estimated eigenvalues to be real—and in fact four of the five estimated eigenvalues are complex.

observed proxies of environmental concerns, confounding factors, and idiosyncratic factors, to verify whether those last two types of factors have been purged from the benchmark greenium.

4.1 Data

The key features of the German green and conventional bonds are retrieved from Refinitiv Eikon. The data comprises the issue date, maturity date, coupons, their frequency, and a tag that indicates whether the bond is green or not. Eikon provides the green label to bonds that were verified by the Climate Bond Initiative (CBI), who created industry-specific standards for bond proceeds to be considered green and in line with the goals outlined in The Paris Climate Agreement. Certified third-party verifiers use the Climate Bond Taxonomy as a benchmark to assess the eligibility of a bond.²⁰ Our pricing data is from Factset; we observe 172,267 daily prices for 164 German bonds (including five green bonds) from October 27, 2008 to January 30, 2023.

4.2 Model Fit

Although the standard practice in the fixed-income literature is to estimate sovereign nominal bond yields using three latent factors (Litterman and Scheinkman, 1991; Cochrane and Piazzesi, 2008), we need four latent factors because we use maturities out to 30 years. The conventional wisdom that three factors are sufficient applies only to bonds with a maximum of 10 years left to maturity, which is the main focus of the vast majority of the DTSM literature, with a few exceptions (e.g., Le and Singleton 2013, Berardi, Brown and Schaefer 2021). However, one of the five German green bonds has 30 years to maturity, and we certainly do not want to lose this observation. Pricing these very long-maturity bonds requires an additional factor, especially later in the sample when the 1–10 year yield-curve slope is steep, but the 10–30 year slope is relatively flat.

²⁰Details on the verification process can be found [here](#).

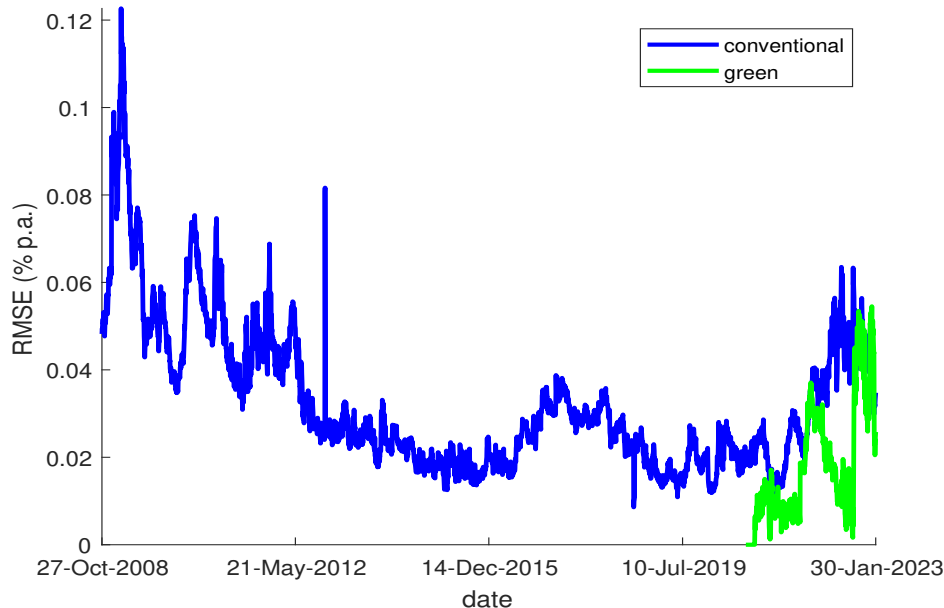


Figure 3. Fit to Conventional and Green Bond Prices

The figure plots the root mean squared error (RMSE) in annualized percent over time for the model in Proposition 1 estimated on the universe of German sovereign bonds. The blue line plots the RMSE for conventional bonds, while the green line plots the RMSE for the five green bonds.

Figure 3 plots the model fit over time in terms of root mean squared error (RMSE); the blue line plots the RMSE for conventional bonds, while the green line plots the RMSE on green bonds. Not surprisingly, as in all DTSMs, the model fit is poorest in late 2008, during the tail end of the financial crisis. The model fit then improves gradually over time, with the RMSE falling to between 1–2 bps by 2015. In early 2023, it has begun to increase again, to 5–6 bps. This is mostly due to the inversion of the yield curves related to the rapid pace of monetary policy tightening.

4.3 Estimated Benchmark Greenium

The blue line in Figure 4 plots the estimate of the German 10-year benchmark greenium; that is, the model-implied yield difference between a 10-year constant-maturity green bond and a 10-year constant-maturity conventional bond. First of all, it is evident that the benchmark

greenium varies significantly over time, a feature that is unveiled because of the use of a dynamic pricing model. This, in turn, will allow us to study the economic and financial drivers of the greenium over time.

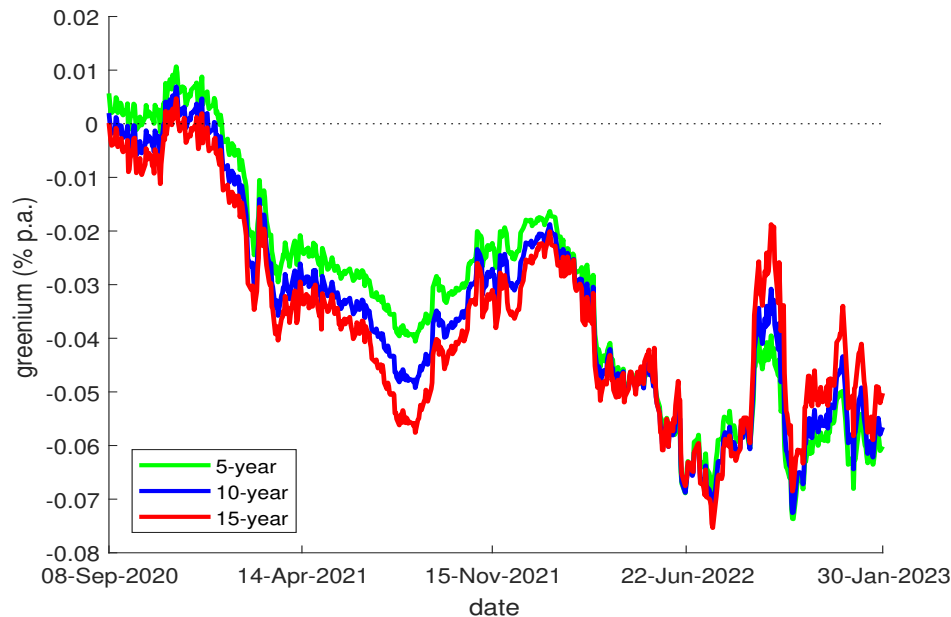


Figure 4. Benchmark Greenium at Various Maturities

The figure plots the model-implied benchmark greenium in annualized percent over time, defined as the yield difference between a zero-coupon green bond and a zero-coupon conventional bond with the same constant maturity over time. The green line plots the 5-year benchmark greenium, the blue line plots the 10-year benchmark greenium, and the red line plots the 15-year benchmark greenium.

Specifically, the model-implied benchmark greenium averages to about 4 basis points over the sample period (3.5% of the average 10-year yield in the sample). In the first few months, it is close to zero; this is driven by the fact that the conventional twin bonds at this time are in fact over-priced, according to the model, by an amount equal to the green spread. Then it increases significantly in the summer of 2021, most likely as investors’ concerns about climate change heightened amid the devastating German floods. Finally, it widens sharply in the last week of February 2022 following a shock to energy prices due to the Ukraine invasion, and it continues to widen reaching a peak of about 7 basis points in the summer of 2022. Interestingly, the model completely disregards the large increase in the shortest maturity

green spread that occurred at year end 2022 and does not attribute it to the benchmark greenium. This is precisely what the DTSM should do when fluctuations are isolated in a single pair of twins, and quickly revert. Those types of fluctuations are likely not related to a systematic green factor that captures wide environmental concerns.

Figure 4 also plots the greenium at the 5- and 15-year maturities to illustrate the properties of the greenium term structure over time. It does not appear to be constant over time: it is slightly upward-sloping at the beginning of the sample (the 15-year greenium is larger than the 5-year greenium); it steepens in the second half of 2021; it flattens again following the start of the war in Ukraine and the related spike in energy prices; and it inverts as the ECB starts tightening monetary policy.

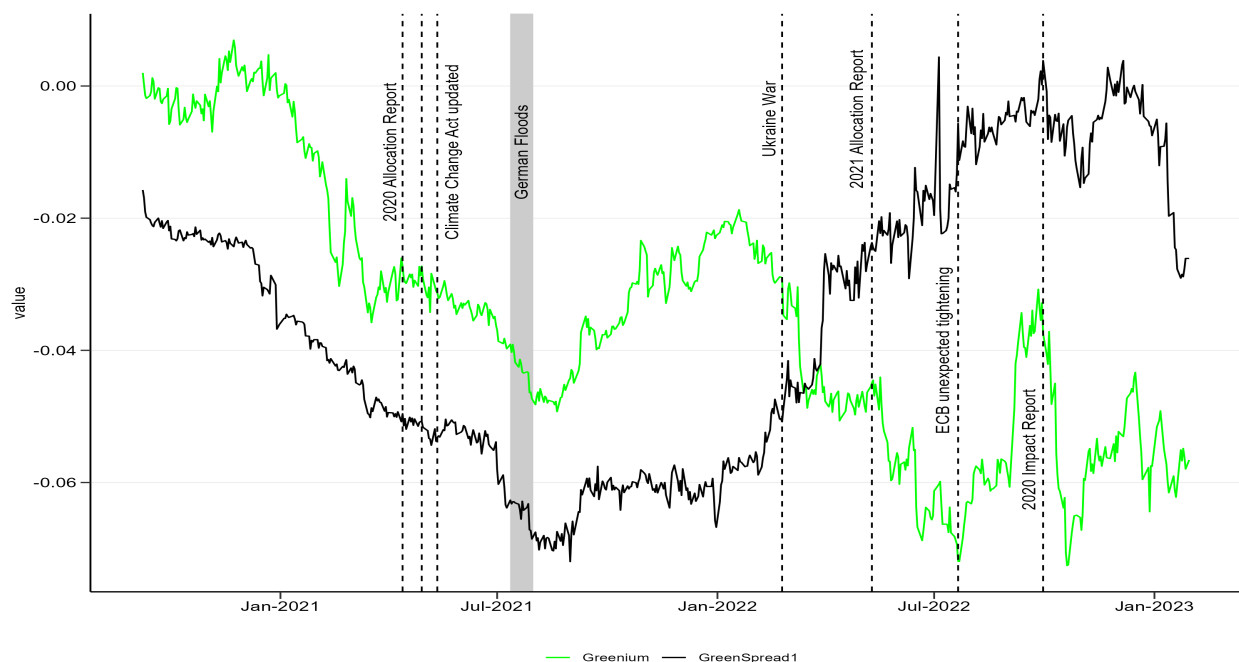


Figure 5. 10-Year Benchmark Greenium and 2030/08/15 Green Spread

The figure plots the model-implied 10-year greenium from Figure 4 (green line) against the green spread for the first pair of German green and conventional bonds from Figure 2 (black line). Both measures are plotted in annualized percent.

This stays in contrast with the downward-sloping term structure of the green spreads, displayed in Figure 2, where starting in September 2021 the 5-year green spread is always larger than the 30-year spread. Actually, by the end of the sample period, the 10- and 30-

year green spreads almost revert to zero, suggesting that, despite the German floods and the spikes in energy prices, at these horizons environmental concerns have diminished rather than increased. This suggests that factors other than environmental preferences have dominated the fluctuations of the green spreads, but not those of the model-implied greeniums.

Finally, we contrast our estimated 10-year constant-maturity benchmark greenium with the green spread on the first pair of twin bonds, which has a similar maturity and the longest time series of the five green spreads. Both are plotted in Figure 5. Although there is a wedge between the two measures, they roughly track each other for the first half of the sample, including in late 2021 when they both widen. However, after the start of the war in Ukraine in February 2022, the green spread narrows while the greenium widens. This occurs at roughly the same time that the German stock market begins to perform poorly, just as oil and gas prices begin to skyrocket. Further, the benchmark greenium also widens following the first Allocation Report and later the first Impact Report. This suggests that ESG investors were willing to increase their subsidy to the government following those reports, which describe how funds were allocated to green projects and quantify their environmental impact.

5 The Drivers of the Benchmark Greenium

To formally analyze what drives a wedge between these two measures, we relate them to various proxies of shocks to environmental preferences, and confounding/idiosyncratic factors unrelated to such preferences. We find that the green spread is correlated with the confounding/idiosyncratic factors, while the benchmark greenium is not. Furthermore, the benchmark greenium is significantly related with proxies of shocks to environmental/climate concerns, but the green spread is not, or is correlated with a counterintuitive sign. This leads us to conclude that our model does seem to “purge” green spreads of most factors unrelated to investor’s environmental preferences. lending credence to the notion that we have uncovered the shadow value of climate concerns.

To proxy for shocks to investors’ environmental preferences, we use oil futures prices and the size of damages directly caused by all major natural disasters in Europe (in billions of U.S. dollars).²¹ The first measure mostly captures the sharp increase in energy prices following the Ukraine invasion, which particularly affected Germany, and may have further stressed the need to reduce the dependence on fossil fuel and accelerate the transition toward clean energy.²² The second measure of shocks to climate concerns is mainly driven by the floods that disrupted Western Europe (principally Germany) in July 2021—marked by the grey area in Figure 5—which led to 236 deaths and over \$40 billion in economic damages.

To proxy for confounding/idiosyncratic factors that drive a wedge between the benchmark greenium and the green spread, we use indicators that capture purely financial motives (such as risk-return trade-offs and flight to quality) as well as demand/supply imbalances between conventional and green bonds. For the former, we use the German stock-market price index (DAX) and the spread between the special collateral (SC) repo rate of German government securities and the average SC repo rate on government securities of other EU countries.²³ This spread measures the special value of German government bonds relative to other European government bonds. When investors prefer the safer and more liquid German government securities, the German SC repo rate will be lower than the average European SC repo rate, hence a negative SC repo spread is a proxy of flight-to-quality. In episodes of high demand for conventional relative to green bonds, we should observe the SC repo spread becoming more negative and green spreads less negative, i.e. an inverse relation. To capture further demand imbalances between green and conventional bonds, we exploit the differences between the net flows into Eurozone-focused fixed-income government-style ESG and non-ESG funds from Morningstar, scaled by the respective total assets under

²¹We obtain the data from the [International Disaster Database EM-DAT](#), which is freely available. The data also includes an estimate of the death toll from each disaster; although this variable lacks the coverage of the economic damages, our results are similar if we use it, instead.

²²We have also used gas prices and obtained the same results not shown for brevity.

²³The data are from Brokertec and cover Belgium, France, Germany, Italy, Netherlands, and Spain. For each country, the SC repo rate is a volume-weighted average of the rates on all the daily special repo transactions.

management (AUM). To capture supply imbalances, we use dummy variables tracking the dates of the auction re-openings for the green and conventional twin bonds.

All of these proxies of flight to quality and relative scarcity may also capture temporary liquidity differentials between conventional and green bonds—which are factors unrelated to environmental preferences.

Finally, we also include a dummy that equals one at the time of the first release of the German impact report (which detailed the impact of green spending on the environment and climate) and a dummy that equals one at the time of the ECB announcement of major steps to expand its climate-related framework (July 4, 2022). All the measures announced on that day might have been perceived as significantly increasing the probability of the ECB shifting its balance sheet and facilities toward greener assets, increasing their value. This, in turn, should translate into a larger benchmark greenium because of the ECB’s regulatory support for green assets. This type of greenium, which we label “regulatory” greenium, could derive from the interaction of environmental preferences with the fundamentals of the economy, in this case the stance of monetary policy. Both dummies are marked by vertical lines in Figure 5.

Figure 6 visualizes the univariate relations between the 10-year model-implied greenium and the green spread with three key proxies: the German stock-market price index (DAX), the EU oil future prices, and the SC repo rate spread. While the green spread is strongly negatively correlated with stock-market prices and the SC repo rate spread, the model-implied greenium is barely affected by stock market prices and has a positive relation with the SC repo rate spread, suggesting that it is not driven by financial motives. For instance, flight-to-quality episodes in which stock prices decline and the SC repo rate spread becomes more negative seem to be associated with a shrinking green spread (less negative), as investors favor the more liquid conventional bonds relative to the green bonds. Such episodes are unrelated to environmental preferences, and indeed the greenium reacts quite differently.

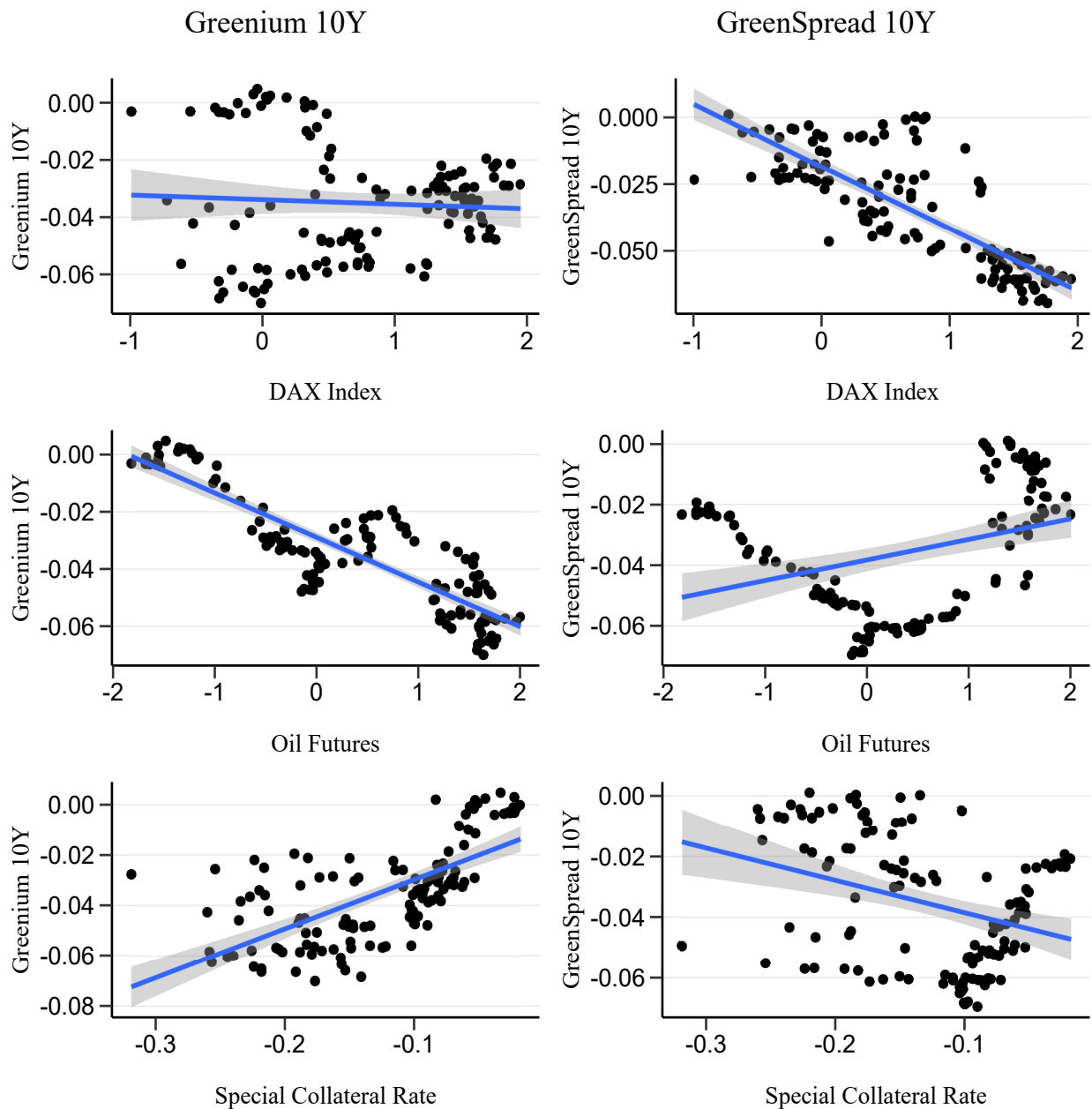


Figure 6. Univariate Relations with Key Variables

The figure plots scatter plots of the 10-year model-implied greenium (left column) and the green spread between the oldest German green bond and its conventional twin (right column) against the German DAX index (first row), the EU Brent Crude Oil Forward (second row), and the Germany-EU SC repo spread (third row). The blue lines report the coefficient estimates, and gray areas denote the 95% confidence intervals, from univariate regressions.

To quantify the relations of the greenium and green spread with all of the proxies described above, and to verify whether the model has indeed purified the greenium from id-

iosyncratic and confounding risk factors unrelated to environmental preferences, we run the following weekly regressions:

$$y_t = \beta_0 + \beta_1 \text{DAX}_t + \beta_2 \text{Oil Fut}_t + \beta_3 \text{SC Repo Diff}_t + \beta_4 \text{Nat Disast}_t + \beta_5 \mathbb{1}(\text{ReopG}) \\ + \beta_6 \mathbb{1}(\text{ReopC}) + \beta_7 \mathbb{1}(\text{ECB}) + \beta_8 \mathbb{1}(\text{ImpactRep}) + \beta_9 \text{Fund Flow Diff}_t + \varepsilon_t, \quad (14)$$

where y_t is either our model-implied 10-year greenium, or the green spread on the oldest German green bond maturing on August 15, 2030. Tables 2 and 3 report the results of estimating equation (14) for the greenium and green spread, respectively. The first three columns in each table report univariate regression results, while the last two columns report the full multivariate results.

Table 2 shows that our estimated greenium is highly correlated with proxies for environmental concerns. The only variables that are stable across regressions and statistically significant are shifts in oil futures and the damages from natural disasters. Moreover, oil futures are by far the most economically significant driver of the benchmark greenium: the increase in the R-squared from adding variables other than oil futures (i.e., going from column 2 to column 5) is quite small.²⁴ Importantly, the estimated coefficients on natural disasters in columns 4–5 imply that the \$40 billion of damages from the German floods explain about 1.2 basis points of the greenium’s average magnitude of 4 basis points.

Jointly, as shown in the last column, the proxies of shifts in environmental/climate concerns and the ECB announcement explain nearly 80% of the variation in the model-implied greenium. We favor this specification to the one reported in column 4 because the SC repo rate spread flips sign across specifications, due to its high correlation with oil prices. Anecdotal evidence suggests that as oil prices jumped following the start of the Ukrainian war, investors used the German bunds to post margin in oil derivatives, increasing specialness spreads on those securities in the repo market (Fortuna et al., 2022).

²⁴We obtain a similar result using gas futures.

	<i>Greenium</i>				
	(1)	(2)	(3)	(4)	(5)
DAX Index	-0.160 (0.243)			-0.107 (0.116)	-0.161 (0.124)
Oil Futures		-1.561*** (0.078)		-2.089*** (0.143)	-1.565*** (0.083)
SC Repo Diff			19.471*** (1.985)	-10.430*** (2.392)	
Natural Disasters				-0.028** (0.013)	-0.029** (0.013)
Reopening Green				-0.077 (0.639)	-0.114 (0.687)
Reopening Conv				0.298 (0.547)	0.267 (0.588)
ECB An. 7/4/22				-1.749** (0.673)	-1.401* (0.718)
Impact Report				0.886 (0.906)	1.336 (0.967)
Net Fund Flows				-23.361 (106.542)	-96.900 (113.004)
N Obs.	126	126	126	126	126
Adjusted R ²	-0.005	0.760	0.432	0.802	0.771

Table 2. Drivers of the Benchmark Greenium

The table reports the results of estimating equation (14) on weekly data from September 8, 2020 to January 27, 2023, including the DAX Index, the natural logarithm of oil futures and the difference in GC repo rates between Germany and the rest of Europe as independent variables. “Natural Disasters” refers to the total economic damages, in billions of U.S. dollars, from all major natural disaster in Europe (from the [International Disaster Database EM-DAT](#)). “Reopening Green” and “Reopening Conv.” are indicator variables for weeks in which the GFA reopened the green bond or its conventional twin, respectively. “ECB An. 7/4/22” is an indicator for the week of July 4, 2022, when the ECB announced major steps to expand its climate-related framework. “Impact Report” is an indicator for the week of the release of the first report on the impact of the green investments. “Net Fund Flows” is the difference in the weekly net flows into ESG and non-ESG funds as percentage of total AUM. *p<0.1; **p<0.05; ***p<0.01.

	<i>Green Spread</i>				
	(1)	(2)	(3)	(4)	(5)
DAX Index	-2.341*** (0.155)			-2.343*** (0.136)	-2.333*** (0.135)
Oil Futures		0.677*** (0.162)		0.834*** (0.167)	0.736*** (0.090)
SC Repo Diff			-10.627*** (2.680)	1.950 (2.789)	
Natural Disasters				-0.016 (0.015)	-0.016 (0.015)
Reopening Green				-1.356* (0.745)	-1.349* (0.744)
Reopening Conv				0.894 (0.638)	0.900 (0.636)
ECB An. 7/4/22				-1.316* (0.785)	-1.381* (0.778)
Impact Report				-0.328 (1.057)	-0.412 (1.047)
Net Fund Flows				64.015 (124.209)	77.763 (122.374)
N Obs.	126	126	126	126	126
Adjusted R ²	0.644	0.117	0.105	0.767	0.768

Table 3. Drivers of the Green Spread

The table reports the results of estimating equation (14) on weekly data from September 8, 2020 to January 27, 2023, including the DAX Index, the natural logarithm of oil futures and the difference in GC repo rates between Germany and the rest of Europe as independent variables. “Natural Disasters” refers to the total economic damages, in billions of U.S. dollars, from all major natural disaster in Europe (from the [International Disaster Database EM-DAT](#)). “Reopening Green” and “Reopening Conv.” are indicator variables for weeks in which the GFA reopened the green bond or its conventional twin, respectively. “ECB An. 7/4/22” is an indicator for the week of July 4, 2022, when the ECB announced major steps to expand its climate-related framework. “Impact Report” is an indicator for the week of the release of the first report on the impact of the green investments. “Net Fund Flows” is the difference in the weekly net flows into ESG and non-ESG funds as percentage of total AUM. *p<0.1; **p<0.05; ***p<0.01.

In contrast, Table 3 shows that the green spread is mostly driven by financial motives. The green spread is significantly correlated with German stocks prices (columns 1, 4, 5, and Figure 1), which by themselves explain 64% of variation in the green spread, as well as with our proxy for flight to quality (columns 3). Worse, the coefficient on oil futures has a counter-intuitive sign, suggesting that as oil prices rise—and investors become more concerned about climate issues—the green spread shrinks towards zero. Further, the green spread is also affected by the re-openings of the green securities, indicating that their supply matters, which is not the case for the greenium. Interestingly, the green spread is not statistically significantly related to the damages from natural disasters—our key proxy for environmental concerns. Finally, the ECB announcement about its climate-related framework is significant for the green spread and the benchmark greenium, indicating that the model has not purged the “regulatory” component of the benchmark greenium.

6 Expected Green Excess Returns

While the benchmark greenium is an object of interest in its own right, the model also allows us to estimate differences in *expected returns* between green and conventional bonds, that is, the expected green excess return. Expected green excess returns are distinct from the greenium analyzed above, because they depend not only on the risk-neutral side of the model, but also on the time-series parameters through equations (2) and (3).²⁵

Not only are the benchmark greenium and expected green excess return different, they can even have opposite signs. Yields are only expected returns from holding bonds to maturity;²⁶ hence, over shorter holding periods, it is possible for expected returns to diverge from yields,

²⁵It is precisely the LG model’s strict separation of time-series and risk-neutral parameters that allows us to make this distinction so cleanly; see [Pancost \(2021\)](#) for further discussion of this point.

²⁶Strictly speaking, this statement is only true for zero-coupon bonds—as four of the five German green and conventional twin bonds happen to be. Once a bond pays coupons, its yield to maturity and expected return to maturity will differ, since the coupon payments must be reinvested at unknown future yields. This difference between expected returns and yields to maturity will be all the more important going forward, as rising interest rates imply that future German bonds will no longer be zero-coupon. Indeed, the fifth German green bond (issued on September 7, 2022) pays a 1.3% coupon.

especially for longer-maturity bonds. In fact, we find that expected green excess returns are often positive, even though the greenium is consistently negative.

The reason that expected green excess returns can be positive, even though the green yield spread is always negative, is because the green utility flow G_t is risky. Suppose first that $G_t = 0$ for all t ; then the green bond and its twin must have the same price, by no arbitrage. Now suppose $G_t > 0$ is known with certainty for all t ; the green bond’s price must be higher—otherwise it would dominate the conventional twin—and the expected excess *pecuniary* returns at any horizon would be negative.²⁷ This is the *discount rate component* of the expected green excess returns: the green bond, by virtue of its intermediate (non-pecuniary) payments, must be discounted at a lower rate than the conventional bond.

Now suppose G_t is risky. The price of the green bond must fall (though not all the way down to the price of the conventional twin), as ESG investors must earn a risk premium to bear this additional risk. This drop in price relative to the deterministic G_t case is the *risk premium* component, and it implies that the expected green excess return is a bit higher than the deterministic case, on average. Generally, the benchmark greenium and expected green excess return are both negative. However, because the risk premium on G_t is changing over time, it can happen over short horizons that the risk premium component is stronger than the discount rate component, so that short-horizon expected green excess returns can be positive even though the greenium is negative. Figure 14 in Appendix D shows how expected green returns vary with the state variable X_t and G_t over short horizons, but not longer ones.

To show how the model-implied expected green excess returns compare to the realized green excess returns in our sample, in Figure 7, we plot

$$100 \times \left[E_t \Delta P_{t+h}(\tau - h) - [P_t^g(\tau) - P_t(\tau)] \right] \quad (15)$$

²⁷Including the utility flow in the definition of the excess return would equalize the excess returns, since G_t is known with certainty. In other words, both expected and realized excess returns on both bonds must be exactly equal if G_t is known with certainty.

where $t + h$ runs along the x -axis, and t is fixed at the first trading date of each bond. Equation (15) is the green excess return earned from an h -period long-short strategy, buying the green bond and financing the purchase by short-selling a conventional bond of the same maturity at time t , and then holding the position for h periods before unwinding it.²⁸ The left panel plots realized vs. expected values of equation (15) for the first German twin bond pair, and the right panel for the second German twin bond pair.

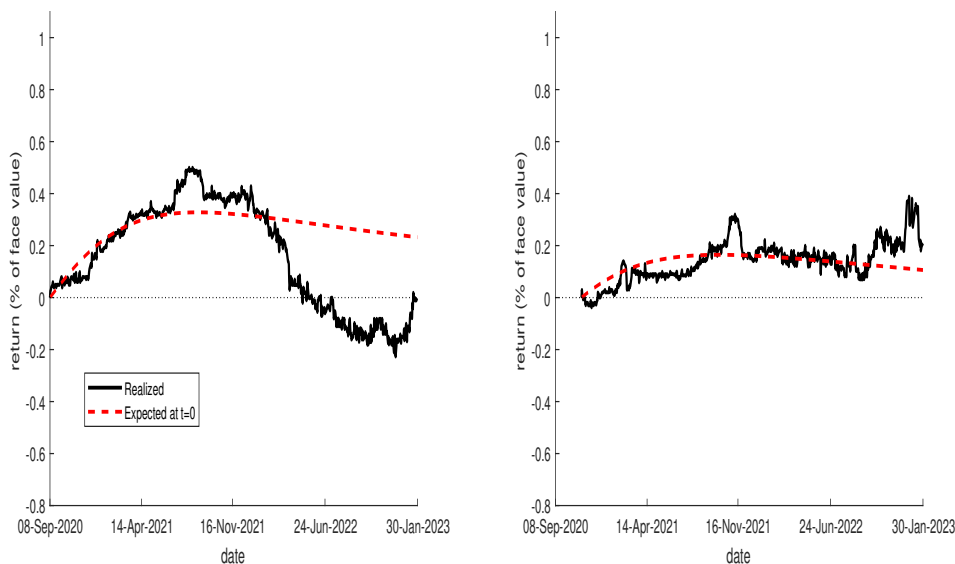


Figure 7. Realized and Expected Green Excess Returns at Issuance

The figure plots the realized cumulative excess returns on two of the four German twin pairs over time, according to equation (15), where t is fixed at the issuance date and $t + h$ runs along the x -axis. The solid black line plots the realized return, while the dashed red line plots the expected return at t .

Figure 7 shows that, for short horizons, the expected green excess returns (red) are positive on the dates when these green bonds were issued. The reason is that the benchmark greenium at this time was quite small (Figure 4), allowing the risk premium component to dominate the discount rate component, which is reasonable given the uncertainty surround-

²⁸Because the model does not price either bond perfectly at t , but the expectations of future prices do not contain any measurement error, we include in our calculation of equation (15) a forecast of the bond-level measurement errors. We estimate that the bond-level pricing residuals from equation (13) have a daily autocorrelation of $\rho \approx 0.99$.

ing a novel security. Further, for both bonds, realized (black) and expected green excess returns are quite close to each other. However, in early May 2021, as Germany’s federal cabinet unexpectedly sets tougher CO2 emission reduction targets after a surprising top court rulings,²⁹ green bonds start performing better than expected. The gap between realized and expected green excess returns increases further following the German floods in July 2021. In other words, as the German government signals a stronger commitment to reduce the impact of climate change and investors become more concerned about its consequences, the prices of green bonds increase relative to conventional bonds.

To verify whether the performance of green bonds relative to conventional bonds is driven by the flow of information described above, in Figure 8, we recompute the expected green excess returns for the first pair of twin bonds starting from after the German floods (September 2021), rather than from the time of issuance (September 2020) as shown in Figure 7. In other words, we ask ourselves how the expected green excess returns change once investors learn about the 2021 Climate Change Act and the German floods and choose to hold green bonds. That is, how much additional expected return are ESG investors willing to forgo (relative to holding conventional bonds) after the new information?

The left panel of Figure 8 shows that after the German floods, expected green excess returns are indeed negative, as predicted by Pastor, Stambaugh and Taylor (2021) and shown by Ardia et al. (2022). Furthermore, realized returns are still a bit higher for the first 6 months, but then sink below the expected returns following the beginning of the Ukrainian war in February 2022. The unexpected invasion of Ukraine most likely pushed investors toward the more liquid conventional bonds, which is typical during flight-to-quality episodes. For this reason, the right panel of Figure 8 shows the expected green excess returns

²⁹On April 29, 2021, the Federal Constitutional Court (Germany’s highest court) rules that the 2019 Climate Change Act was unconstitutional because of generational equity violation. Even if the German government had until the end of 2022 to amend the 2019 Climate Change Act, on May 12, 2021, Germany’s federal cabinet adopts the reforms to the 2019 Climate Change Act, that is, the 2021 Climate Change Act shifts to a net-zero target by 2045. See The Economist “A court ruling triggers a big change in Germany’s climate policy”; POLITICO “Top German court rules the country’s climate law is partly ‘unconstitutional’”; Reuters “Germany sets tougher CO2 emission reduction targets after top court ruling.”

for the same pair of twin bonds, but computed starting in March 2022, soon after the invasion of Ukraine. In this case, again, the expected green excess returns are negative, and the green bonds perform worse than expected because of the flight-to-quality to conventional securities. This is consistent with the green spread shrinking due to confounding factors unrelated to environmental preferences.

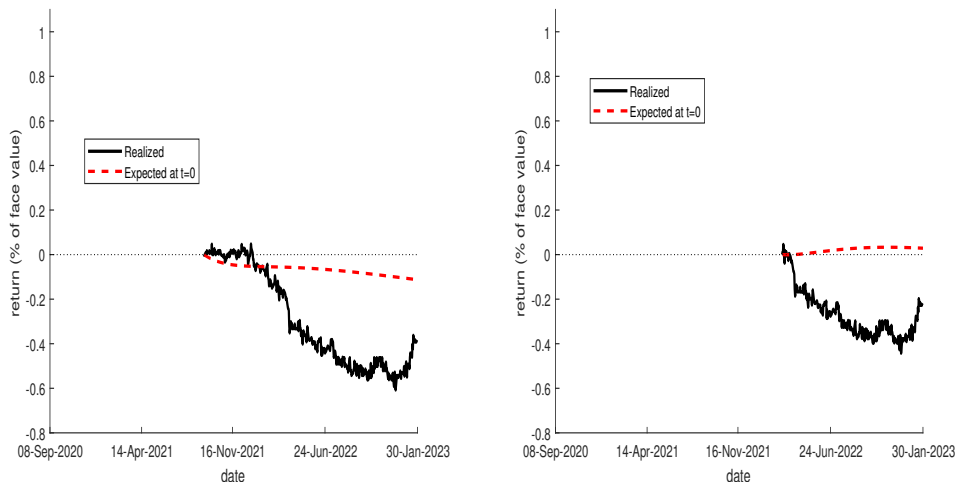


Figure 8. Green Excess Returns after the German Floods

Both panels plot realized and expected excess returns on the first German twin pair. The left panel plots realized and expected returns starting from September 9, 2021 (after the German floods) while the right panel plots realized and expected returns starting from March 1, 2022 (after the start of the war in Ukraine).

We close this section with an illustration of the dynamics and term structure of the model’s expected green excess returns. To do so, in Figure 9, we plot equation (15) over time for a fixed holding period h and maturity τ . In particular, we set $\tau = 10$ years and consider holding periods of 1 month, 1 year, 5 years, and 9 years. This is just one of the possible forecasting exercises that can be conducted with our DTSM.

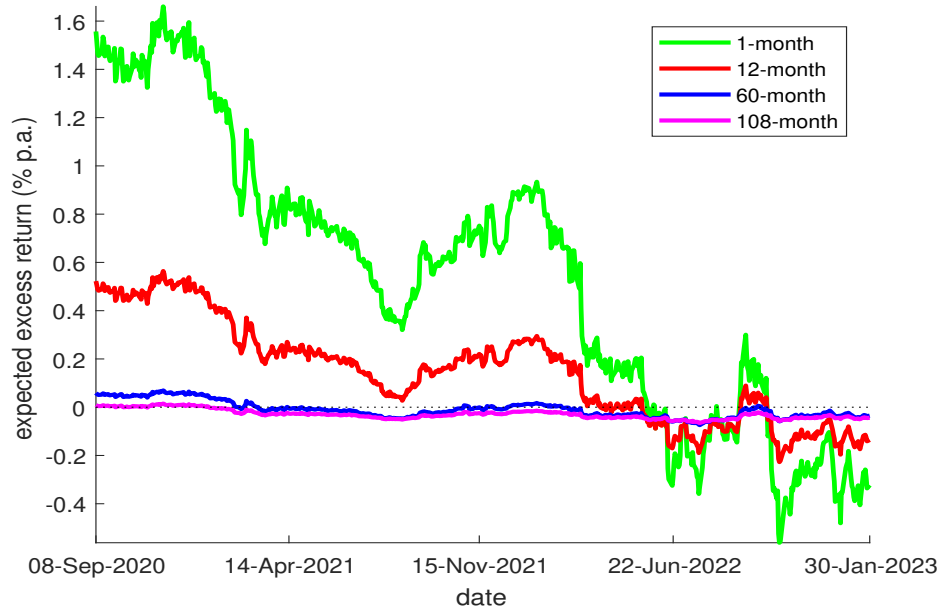


Figure 9. Expected Green Excess Green Returns at Various Horizons
 The figure plots the model-implied annualized expected green excess returns from equation (15) for a 10-year bond over holding periods of 1 month, 1 year, 5 years, and 9 years.

Figure 9 shows that the model-implied expected 1-month green excess returns (green) can be either positive or negative, can change quite rapidly, and have been decreasing steadily over the sample—as the benchmark greenium has gotten larger (Figure 4). In addition, while expected green excess returns can be large and positive over short horizons, as the horizon increases they converge to the greenium, which is the return from holding to maturity (and is negative in our sample). Early in the sample—when green spreads are widening—expected green excess returns are positive, though not constant. In mid-2021, after the German floods, expected green excess returns narrow and then bounce back before becoming negative. Around March 2022—after the beginning of the war in Ukraine—expected green excess returns turn into negative territory, where they largely remain until the end of the sample.

7 Robustness

To estimate the benchmark greenium, our baseline model includes an extra factor (G_t) dedicated only to green bonds. As a result, the fitting errors on green bonds are smaller than those on conventional bonds (Figure 3). The implicit assumption (which is also necessary for using the green spread) is that conventional twin prices align with the prices of all other conventional bonds, and therefore do not need an extra factor dedicated to them. However, if this assumption is incorrect, and we do not include a pricing factor specific to conventional twins, then their mis-pricing could bias our estimated conventional yield curve, and through it the benchmark greenium.

To verify whether this is the case, we proceed in steps. First, we demonstrate that conventional twin bonds are not representative of the German conventional yield curve. Second, we address this issue by augmenting the model with an additional “twin” factor that prices only conventional twins, and we use this augmented model to re-estimate the benchmark greenium. This allows us to estimate a conventional yield curve that is not affected by the risk characteristics specific only to conventional twins. It has also the additional benefit of putting the green and conventional twins on the same footing—each will be priced with an additional factor—reducing the likelihood of over-fitting green bonds relative to their conventional twins.³⁰

Table 4 reports the baseline model fit (measured by the average price residuals) at various maturities obtained using either all securities or only conventional twins. In particular, the first row reports average price residuals for the model estimated on the full sample period of conventional bonds. The other rows report results from models with the same risk-neutral parameters θ^* , but estimated after September 9, 2020—the issuance date of the first green bond. In the row labeled “All Bonds,” we estimate the factors X_t using all available bond prices; while, in the row labeled “Twins Only,” the factors are estimated to price the five

³⁰Recall that in the baseline model the green securities are priced using 5 factors, as they have the green factor (G_t) dedicated only to them; while, conventional twins are priced using 4 factors like any other conventional security.

conventional twins without error, but still pricing all available bonds.

Model	Maturity Range					
	All	< 3	[3, 5)	[5, 10)	[10, 15)	≥ 15
Full Sample from Sept 2020	0.000548	0.0017	-0.000899	0.00349	-0.0101	-0.000719
All Bonds	5.31e-05	-1.07e-05	-0.00661	0.0077	-0.0313	0.00377
Twins Only	0.0368	0.14	0.00863	-0.000971	-0.0162	-0.00278

Table 4. Model Fit

The table reports average residuals in annualized percent for various models and for bonds of different maturities. The residuals are defined as actual minus model-implied price, scaled by duration, and are thus in units of annualized percent. The first column reports the overall statistic; subsequent columns report statistics for bonds with less than 3, 3–5, 5–10, 10–15, and greater than 15 years remaining maturity, respectively. The first row reports results for the full sample; subsequent rows report results for the sample restricted to post September 9, 2020 (i.e., when the first green bond appears in the data). The row labeled “All Bonds” uses all bonds on this sub-sample; the row labeled “Twins Only” reports results in which the factors X_t are estimated to closely match the prices of the conventional twin bonds.

Overall, Table 4 shows that the conventional twins are not representative of the entire conventional yield curve. A model focusing only on twin yields, which all have medium to long maturities, leads to biased estimates of bond prices, mostly due to the extreme overpricing of securities at the short end of the yield curve, since there are not (yet) any green and conventional twins with less than 3 years left to maturity. This reinforces the importance of including all conventional bonds in the estimation; but also, that the model might benefit from an additional factor dedicated to the conventional twins themselves.

To explore whether our benchmark greenium estimation is affected by the mis-pricing of the conventional twins, we re-estimate our model with an additional “twin” factor, T_t . In this augmented model, conventional non-twin bonds are priced with four latent conventional factors, the five green bonds are priced using the four conventional factors and G_t , and the five conventional twin bonds are priced using the four conventional factors and T_t .

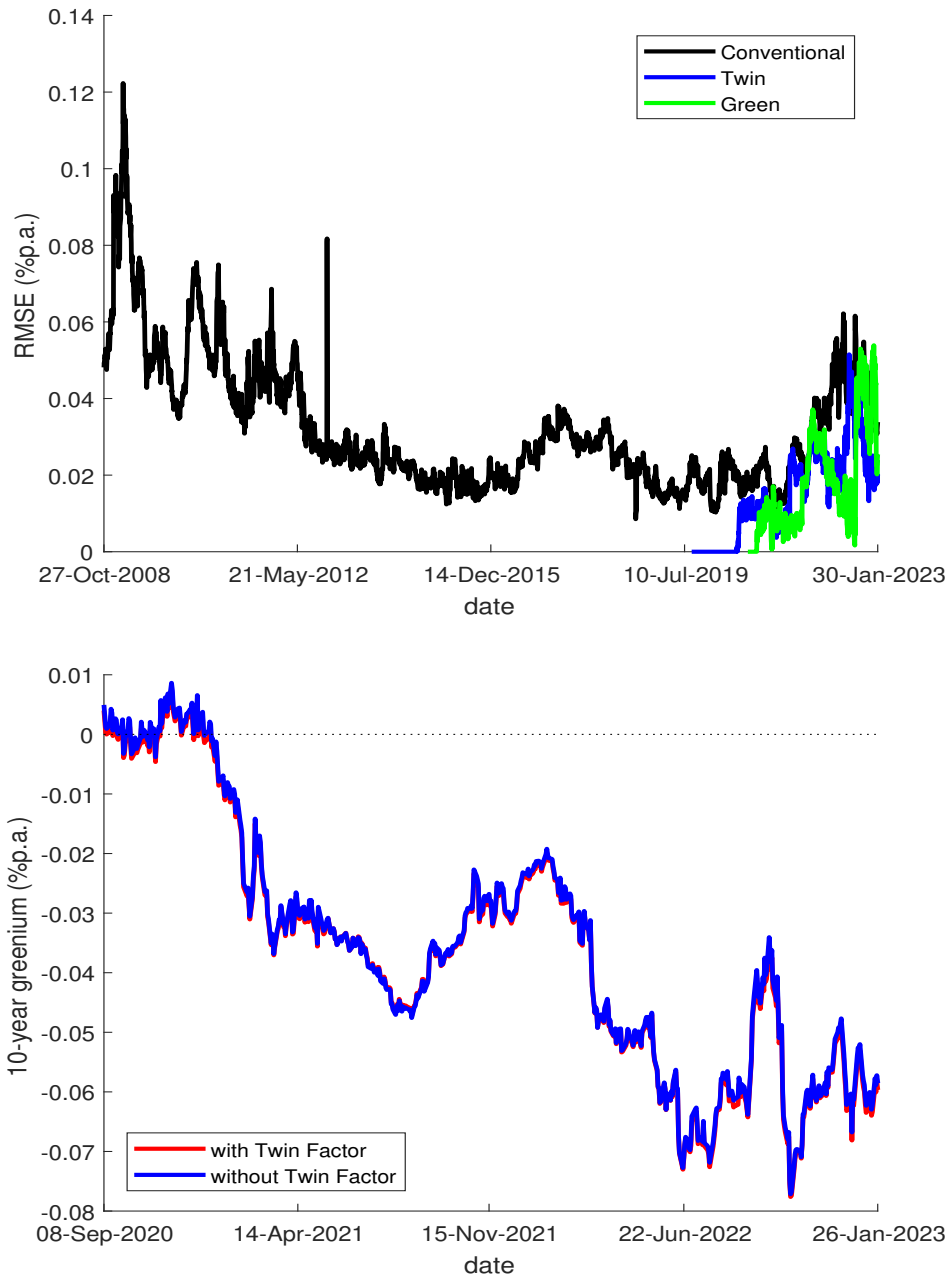


Figure 10. Model Fit and Benchmark Greenium with Additional Twin Factor
 The top panel plots the root mean squared error (RMSE) in annualized percent over time for the extended model in which twin bonds have an additional free factor similar to the green bonds. The black line plots the RMSE for conventional (non-twin) bonds, the blue line plots the RMSE for the five conventional twin bonds, and the green line plots the RMSE for the five green bonds. The bottom panel plots the model-implied 10-year benchmark greenium from the extended model in annualized percent as a red line and the 10-year greenium from the benchmark model (i.e. the blue line in Figure 4) is plotted in blue for comparison.

The top panel of Figure 10 plots the root mean-squared error (RMSE) over time for this augmented model. Now, the fitting errors of the green bonds and their conventional twins are similar, once there are multiple green and twin bonds in the sample. For the portion of the sample where there is only a single observed twin price, the single twin factor sends the RMSE to zero by construction. Notice also that the first observed twin bond price in August 2019 appears well in advance of the first green bond price (see Table 1).

However, the bottom panel of Figure 10 shows that having a less parsimonious model of twin bond prices does not affect the benchmark greenium estimate. The red line plots the 10-year benchmark greenium from the augmented model, in which the conventional twins are priced with their own additional factor, while the blue line plots the baseline 10-year benchmark greenium estimate (from Figure 4). The two lines are not identical, but they are virtually indistinguishable from one another. Therefore, we favor the baseline model which is more parsimonious.

Finally, we have conducted additional robustness exercises, including estimating the model with 3, 4, and 5 conventional factors (to price all conventional bonds) and dropping short-maturity (2- and 3-year) bonds from the sample. These changes to our methodology did not affect our baseline estimates, and so for brevity we omit them.

8 Conclusion

We estimate the benchmark greenium by exploiting the unique “twin” structure of German sovereign green bonds. Since the simple yield spread between a green security and its conventional twin (i.e., the green spread) can be contaminated by idiosyncratic and confounding factors unrelated to climate/environmental concerns, we use a DTSM that jointly prices the entire universe of German green and conventional bonds. The model, by estimating the systematic conventional factors driving all bond prices as well as a green factor specific to green bonds, allows us to eliminate temporary mispricing due to idiosyncratic and confound-

ing factors, such as relative scarcity induced by flight-to-quality episodes. In this sense, the model delivers an estimate of the benchmark greenium: the dividend investors are willing to forgo to subsidize the government's green projects.

Indeed, we find that, differently from the simple green spread, the model-implied greenium is uncorrelated with proxies of confounding and idiosyncratic factors. The time-series fluctuations of the estimated greenium are significantly related to major environmental events, while the green spread is mostly driven by market frictions, such as measures of flight to quality and liquidity. Hence, our estimates of the benchmark greenium provide a cleaner measure of the shadow value of wide environmental concerns, and as such give a clearer signal to policy makers currently considering to broaden support for sustainable finance by, for example, including green bonds in the implementation of fiscal and monetary policies.

Further, estimating a DTSM enhances our understanding of the greenium beyond the simple green spread in three ways. First, the benchmark greenium is larger than the raw green spread, highlighting the importance of controlling for security-level mispricing. Second, the model-implied term structure of the greenium is mostly flat, in contrast to the term structure of green spreads which is mostly downward sloping. Third, the model allows us to estimate ex-ante expected returns at all horizons, while green spreads offer only a measure of realized returns and expected returns holding to maturity.

Our estimated expected green excess return (i.e., the difference between expected green and conventional returns) varies with the investment horizon and investors' information set, as it is positive at issuance (September 2020) and turns negative after the German floods (July 2021). In line with [Pastor, Stambaugh and Taylor \(2021\)](#), as investors become more concerned about the environment, they are willing to accept lower returns to hold green assets. Further, as suggested by [Pastor, Stambaugh and Taylor \(2022\)](#), the expected and realized green excess returns diverge when there is an unanticipated increase in climate concerns; but, they also diverge when there are surprises unrelated to environmental preferences,

such as the start of the Ukrainian war that triggered flight-to-quality to German conventional securities. This finding is consistent with a green spread that, differently from the benchmark greenium, is contaminated by market frictions.

Although German public debt has a risk profile very similar to the U.S. public debt and provides an ideal testing ground because of the novel twin structure of the green bonds, we cannot rule out that our greenium estimates are Germany-specific. In particular, if markets are sufficiently segmented, our results might not be perfectly transferable to investors in other countries. However, investors across many geographic areas participate in the market for German federal securities, making this setting at least informative about international preferences for green assets. Another limitation of our focus on Germany is the short time series and the somewhat limited cross-section of green bonds. While the first issue is unavoidable, we note that Germany has issued more green bonds than any other government.³¹ And, not only has Germany issued more green bonds than any other government, but its green bonds cover the full span of maturities, from five to thirty years.

In the future, we can extend our methodology to estimate the greenium for other countries and supranational entities, including France and the UK that issue green bonds but do not pair them directly with a conventional “twin.” Doing so would allow us to extend both the time-series and cross-sectional dimensions of our data. However, adding other countries would involve additional complications, including estimating additional X_t processes (and parameters) to match their conventional yield curves, as well as potentially separate parameters governing their G_t processes.³²

An additional extension would be to use our estimates to analyze the relationship between the primary and secondary market for green bonds, in order to better connect the high demand for green bonds at auction with the dynamics of the subsequent benchmark greenium

³¹As of this writing, France and the U.K. have both issued two green bonds, and the Netherlands, Italy, Spain, Denmark, and Belgium have issued a single green bond each.

³²We could motivate the assumption of a single G_t process across countries governing time-variation in green preferences, despite the differences across countries in the environmental impact of their green investments, with the evidence in Heeb et al. (2023) that green investors appear to be willing to pay for impact, but not significantly more for more impact.

in the secondary market. It may be that the benchmark greenium varies with the composition of investors: for instance, [Pietsch and Salakhova \(2022\)](#) find that in Europe the greenium for corporate bonds gets larger when the share held by retail investors increases relative to the share of investment funds, insurance companies and pension funds.

A Green Bond Market

The green bond market is growing rapidly, and Germany is at the forefront. Green bonds are a subset of ESG investing and are the largest category of ESG fixed income, with \$620 billion issued in 2021 (about 40% of the total ESG issuance), reaching a cumulative amount of \$1.8 trillion worldwide since the inception of the green bond market in 2008 (according to Bloomberg NEF data).

Germany is the second-largest issuer of sovereign green bonds. The top panel of Figure 11 plots cumulative public issuance of green bonds over time for the nine countries that are the largest issuers and for supranational entities, such as the European Union (EU) and World Bank. The European Union (EU) is expected to dominate the green bond supply following its entrance in the market in the last quarter of 2021, as it is committed to issue up to 250 billion euros by the end of 2026.³³

Nevertheless, green bonds remain a relatively limited component of the sovereign bond universe. In particular, as shown in the bottom panel of Figure 11, green bonds typically comprise only 1-4% of outstanding bonds even for the most prolific green issuers.

Demand for German green bonds tends to be high. The first three green bonds were more than six times over-subscribed, and all green bonds have subsequently been re-opened to increase their initial issuance. The investor base for green securities is quite broad, with real money investors accounting for the largest share. In particular, at the 10- and 30-year syndicates, asset managers, central banks, as well as insurance and pension funds acquired between 75 and 90 percent of the issuance.

The German government made substantial green investments before issuing green securities (12.3 billion euros in 2019), and those investments accelerated in 2020 and 2021, totaling indicatively 30.3 billion euros. Its total green bond issuance from September 2020 until June 2022 accumulates to 31 billion euros, therefore making a significant contribution to the total German budget used for environmental projects.

³³See https://ec.europa.eu/commission/presscorner/detail/en/qanda_21_5211.

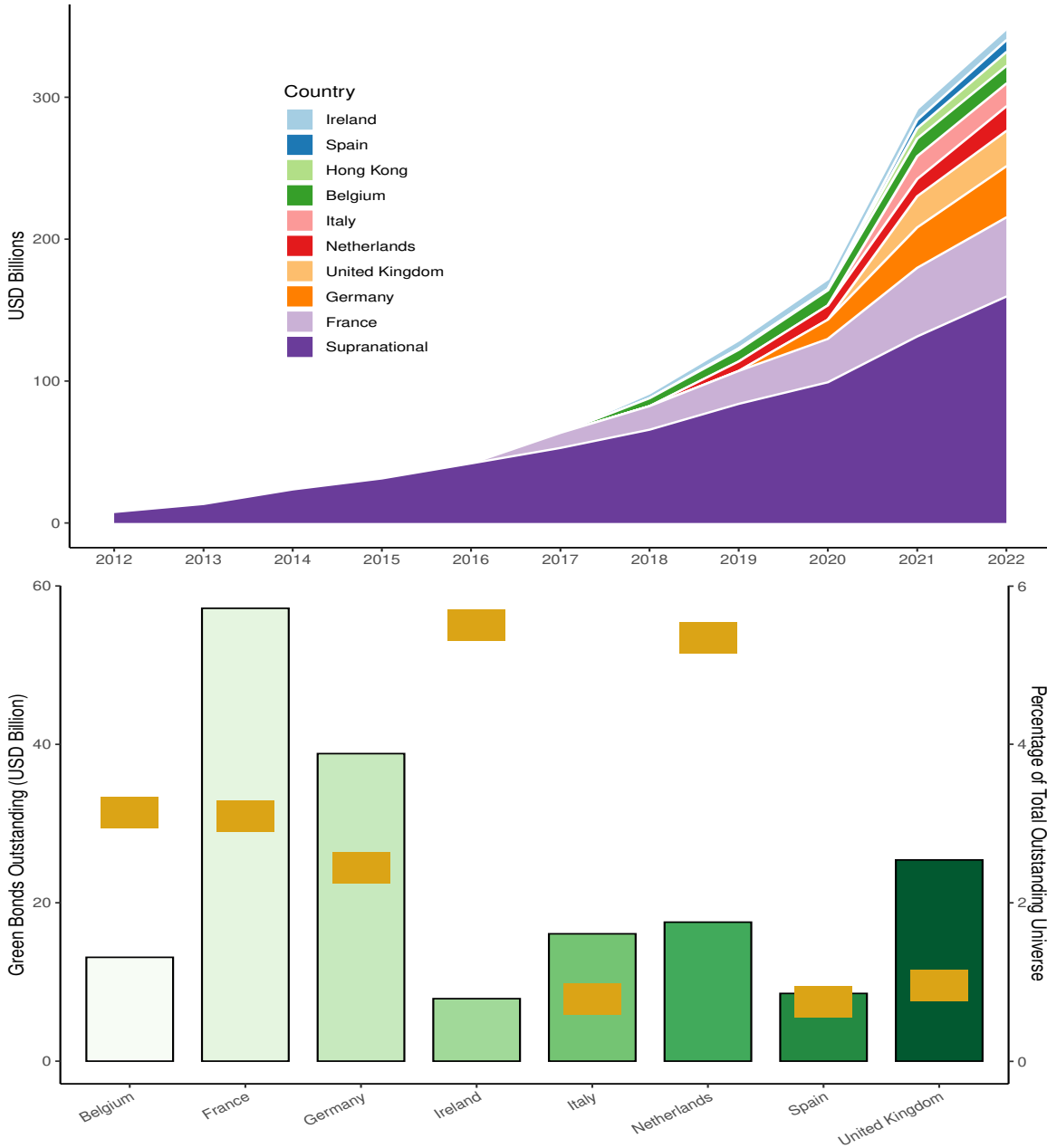


Figure 11. Cumulative Public Green Bond Issuance

The top panel plots cumulative public green bond issuance in billions of dollars per year. The bottom panel plots total sovereign green bond issuance in billions of dollar for the most prolific issuers and as percentage of the total debt outstanding (yellow rectangles). (Source: Bloomberg NEF).

The Green Bond Framework lists five main green expenditure categories that can be assigned to the green federal securities: transport; international cooperation; research, innovation and awareness raising; energy and industry; and agriculture, forestry natural landscapes

and biodiversity. So far, between 50% and 55% of the expenditures has been allocated to sustainable transportation, such as rail, public and non-motorised transportation, electromobility and alternative fuels (especially hydrogen), as transport-related emissions should be cut significantly by 2030. Between 8% and 15% of the expenditures has been allocated to the energy and industry sectors, as Germany aims for full decarbonisation by 2045 through a gradual transformation of the energy supply toward more renewable energies and energy efficiency. About 20% has been used for international cooperation, that is, mostly funding programs and projects targeted at mitigating and adapting to climate change, transitioning towards sustainable energy systems based primarily on renewable energy sources, protecting habitats and biodiversity. Finally, 8% has been used for research and about 5% for sustainable agriculture (e.g., sustainable farming, conservation and sustainable management of forests and timber use, avoiding food waste).³⁴

B Proofs

Proof of Proposition 1

Proof. Define

$$\tilde{X}_t \equiv \begin{bmatrix} X_t \\ G_t \end{bmatrix}$$

and note that equations (2) and (3) imply that

$$d\tilde{X}_t = \left[-\mu - \phi\tilde{X}_t \right] dt + \Sigma d\tilde{W}_t$$

³⁴See slide 25 of Deutsche Finanzagentur (2022), available [here](#).

where

$$\begin{aligned}
W_t &\equiv \begin{bmatrix} W_t^x \\ W_t^g \end{bmatrix} \\
\mu &\equiv \begin{bmatrix} \mu_x \\ \mu_g \end{bmatrix} \\
\phi &\equiv \begin{bmatrix} \phi_x & \vec{0} \\ \vec{0} & \phi_g \end{bmatrix} \\
\Sigma &\equiv \begin{bmatrix} \Sigma_x & \vec{0} \\ \vec{0} & \Sigma_g \end{bmatrix}.
\end{aligned}$$

Similarly, equation (4) can be rewritten as

$$\frac{dM_t}{M_t} = - \left[\delta_0 + \tilde{\delta}'_1 \tilde{X}_t \right] dt - \left[\sigma \left(\tilde{X}_t \right) - \Sigma^{-1} \tilde{X}_t \tilde{X}'_t \tilde{\delta}_1 \right] \cdot d\tilde{W}_t$$

where $\tilde{\delta}_1 \equiv [\delta'_1, 0]'$ and $\sigma \left(\tilde{X}_t \right) = \sigma \left(X_t, G_t \right)$.

Assuming a solution of the form (10) and applying Ito's lemma to the above equations and equation (6) gives

$$\begin{aligned}
0 &= - \frac{\partial \tilde{A}^g}{\partial \tau} - \frac{\partial \tilde{B}^{g'}}{\partial \tau} \tilde{X}_t - \left(\tilde{A}^g(\tau) + \tilde{B}^g(\tau)' \tilde{X}_t \right) \left(\delta_0 + \tilde{\delta}'_1 \tilde{X}_t \right) \\
&\quad + \tilde{B}^g(\tau)' \left[-\tilde{\mu}^* - \tilde{\phi}^* X_t + \Sigma \sigma \left(\tilde{X}_t \right) \right] \\
&\quad - \tilde{B}^g(\tau)' \Sigma \left[\sigma \left(\tilde{X}_t \right) - \Sigma^{-1} \tilde{X}_t \tilde{X}'_t \tilde{\delta}_1 \right] - \delta'_g \tilde{X}_t \left(\delta_0 + \tilde{\delta}'_1 \tilde{X}_t \right) \\
&\quad + \delta'_g \left(-\tilde{\mu}^* - \tilde{\phi}^* \tilde{X}_t + \Sigma \sigma \left(X_t \right) \right) - \delta'_g \Sigma \left[\sigma \left(\tilde{X}_t \right) - \Sigma^{-1} \tilde{X}_t \tilde{X}'_t \tilde{\delta}_1 \right] \\
&= - \frac{\partial \tilde{A}^g}{\partial \tau} - \tilde{A}^g(\tau) \delta_0 - \left(\tilde{B}^g(\tau) + \delta_g \right)' \tilde{\mu}^* - \frac{\partial \tilde{B}^{g'}}{\partial \tau} \tilde{X}_t - \tilde{A}^g(\tau) \tilde{\delta}'_1 \tilde{X}_t - \left(\tilde{B}^g(\tau) + \delta_g \right)' \left(\delta_0 I + \tilde{\phi}^* \right) \tilde{X}_t
\end{aligned} \tag{16}$$

where $\delta_g \equiv \left[\vec{0}_{1 \times k}, 1 \right]'$.

Because equation (16) must hold for all values of \tilde{X}_t , it must be that $\tilde{A}^g(\tau)$ and $\tilde{B}^g(\tau)$ satisfy the system of ordinary differential equations

$$\begin{aligned}\frac{\partial \tilde{A}^g}{\partial \tau} &= -\delta'_g \tilde{\mu}^* - \tilde{A}^g(\tau) \delta_0 - \tilde{B}^g(\tau)' \tilde{\mu}^* \\ \frac{\partial \tilde{B}^{g'}}{\partial \tau} &= -\delta'_g (\tilde{\phi}^* + \delta_0 I) - \tilde{A}^g(\tau) \tilde{\delta}'_1 - \tilde{B}^g(\tau)' (\tilde{\phi}^* + \delta_0 I),\end{aligned}\tag{17}$$

with initial conditions $\tilde{A}^g(0) = 1$ and $\tilde{B}^g(0) = \vec{0}_{k+1 \times 1}$. Equation (11) is the solution of this system, where the top row is the constant function $f(\tau) = 1$ and subsequent rows have been converted from \tilde{X}_t to $\{X_t, G_t\}$ notation.

Equation (8) can be derived as a special case with $\mu_g^* = \phi_g^* = 0$ and $\delta_g = \vec{0}$.

C Additional Estimation Details

In this section we describe in more detail how we estimate the model of Section 3 on the data.

We estimate the models using the SR filter of [Andreasen and Christensen \(2015\)](#), which consists of a two-stage procedure: first, we estimate the risk-neutral parameters θ^* and the latent factors X_t and G_t as described below in Section C.1. Denote the estimated values of X_t and G_t as \hat{X}_t and \hat{G}_t , respectively, so that

$$\begin{aligned}\hat{X}_t &= X_t + \nu_t^x \\ \hat{G}_t &= G_t + \nu_t^g.\end{aligned}\tag{18}$$

where ν_t^x and ν_t^g are sampling errors from the filter. In the first step, we recover the daily covariance matrices Ξ_t^x and Ξ_t^g of ν_t^x and ν_t^g . In the second step, described below in Section C.2, we use these covariance matrices to estimate the time-series parameters of the model, accounting for the estimation of the latent factors and the risk-neutral parameters themselves. To do so, we discretize equations (2) and (3) and treat the time-series side of

the model as a pair of daily vector autoregressions.

To estimate both conventional and green bond prices, accounting for the fact that our samples consists of 172,267 price observations on 164 conventional bonds from October 27, 2008 to January 30, 2023 and 2,042 price observations on 5 green bonds from September 8, 2020 to January 30, 2023, we proceed in steps. First, we estimate δ_0 and μ^* using the longer conventional bond sample only. We then estimate μ_g^* and ϕ_g^* using all bonds, but only the sample starting in September 2020, and holding δ_0 and μ^* fixed. Finally, we estimate all the risk-neutral parameters jointly over the entire sample using the previous two estimates as an initial guess.³⁵

Once we have the seven risk-neutral parameters and the associated estimates for the latent factors, we then estimate the time-series parameters and all standard errors. Table 5 reports the estimated parameters, with standard errors below each value in parentheses.

C.1 Risk-Neutral Parameters

The risk-neutral estimation is a nonlinear least squares (NLLS) problem in the risk-neutral parameters θ^* , where the latent factors are nuisance parameters. Given θ^* , we construct the measurement matrices of equation (13) on each date using the coupon schedule of each bond and the factor loadings of equations (8) and (11). We then estimate \hat{X}_t and \hat{G}_t on each date using equation (13), and compute the total sum of squared residuals across all dates. Finally, we search over values of θ^* to minimize this sum of squared residuals.

The standard errors of θ^* correspond to the usual NLLS standard errors. Let

$$\mathcal{X}_i \equiv \begin{bmatrix} \frac{\partial \hat{P}_i}{\partial \theta_1^*} & \frac{\partial \hat{P}_i}{\partial \theta_2^*} & \dots & \frac{\partial \hat{P}_i}{\partial \theta_k^*} \end{bmatrix} \quad (19)$$

denote the vector of derivatives of the i th estimated bond price with respect to the k risk-

³⁵Because there are only five green bonds and only for a short part of the sample, and because the green bond parameters have no effect on conventional bonds, the parameter estimates in the third step are nearly identical to the initial guess.

δ_0		$\mu^{*'} $		
0.00164 (1.5e-17)	-1.86e-06 (2.68e-20)	6.16e-10 (2.54e-23)	-1.25e-13 (1.29e-26)	1.71e-18 (2.87e-30)
μ		ϕ		
-3.18e-06 (5.17e-06)	-0.00117 (0.00168)	0.00112 (0.00325)	-0.00275 (0.00275)	-0.00213 (0.00414)
3.07e-06 (1.22e-05)	-0.00432 (0.00368)	-0.0178 (0.00796)	0.0131 (0.00659)	0.025 (0.00997)
-3.65e-06 (1.49e-05)	0.00368 (0.00453)	0.0118 (0.00966)	-0.011 (0.0082)	-0.0157 (0.0124)
4.47e-06 (1.21e-05)	-0.00254 (0.00362)	-0.011 (0.00783)	0.0086 (0.00664)	0.014 (0.01)
$\Sigma_x \Sigma'_x$				
	1.01e-12 (3.2e-13)	-1.12e-12 (3.98e-13)	7.19e-13 (4.84e-13)	-8.14e-13 (3.93e-13)
	-1.12e-12 (3.98e-13)	5.13e-12 (2e-12)	-5.13e-12 (1.21e-12)	4.71e-12 (9.85e-13)
	7.19e-13 (4.84e-13)	-5.13e-12 (1.21e-12)	8.12e-12 (2.95e-12)	-6.13e-12 (1.2e-12)
	-8.14e-13 (3.93e-13)	4.71e-12 (9.85e-13)	-6.13e-12 (1.2e-12)	5.2e-12 (1.94e-12)
μ_g^*	ϕ_g^*	μ_g	ϕ_g	Σ_g^2
-7.68e-06 (5.96e-18)	-0.000119 (2.24e-16)	-0.000353 (0.000161)	-0.00674 (0.00276)	5.78e-08 (2.25e-08)

Table 5. Parameter Estimates

The table reports the estimated parameters of the model described in Section 3.1. The top panel reports the risk-neutral parameters that affect all bonds, the second panel reports the time-series parameters μ and ϕ for the conventional factors X_t , while the third panel reports the variance-covariance matrix of the conventional factor time-series residuals. The bottom panel reports both the risk-neutral and time-series parameters affecting green bonds.

neutral parameters, including the parameters that affect green bond prices. For observations i before the introduction of green bonds we set the relevant elements of \mathbb{X}_i to zero. We approximate Equation (19) using a complex-step derivative with step size 10^{-12} .

Let \mathbb{X}_t denote the $n_t \times k$ matrix of stacked derivatives, for the n_t price observations at t , and let \mathbb{X} be the $N \times k$ stacked derivatives across all cross-sections, where $N = 166,680$. Then the asymptotic covariance matrix of θ^* is given by

$$\text{asymVar}(\theta^*) = \frac{1}{N} \left(A^{\theta^*} \right)^{-1} B^{\theta^*} \left(A^{\theta^*} \right)^{-1}, \quad (20)$$

where

$$\begin{aligned} A^{\theta^*} &\equiv \frac{1}{N} \mathbb{X}' \mathbb{X} \\ B^{\theta^*} &\equiv \frac{1}{N} \mathbb{X}' \Sigma_M \mathbb{X} \end{aligned}$$

and

$$\begin{aligned} \Sigma_M &= \text{diag} \left\{ \hat{\Sigma}_t^M \right\} \\ \hat{\Sigma}_t^M &\equiv \frac{1}{n_t} \sum_{i=1}^{n_t} \hat{\varepsilon}_{i,t}^2 \end{aligned}$$

is the maximum-likelihood estimator of the specification-error variance in Equation (13), diagonalized to have the proper dimensionality.

C.2 Time-Series Parameters

While the risk-neutral parameter estimation is a relatively straightforward NLLS exercise, estimating the time-series parameters requires a bit more work. In particular, in the second step we need to account for both the sampling error in the latent factors, as well as the sampling error in the risk-neutral parameters themselves.

First, we discretize the time-series equations (2) and (3) as

$$\begin{aligned} Y_{t+\Delta_t} &\equiv \frac{X_{t+\Delta_t} - X_t}{\sqrt{\Delta_t}} \approx \mu_x \sqrt{\Delta_t} + \phi_x \sqrt{\Delta_t} X_t + \Sigma_x \frac{W_{t+\Delta_t}^x}{\sqrt{\Delta_t}} \\ Y_{t+\Delta_t}^g &\equiv \frac{G_{t+\Delta_t} - G_t}{\sqrt{\Delta_t}} \approx \mu_g \sqrt{\Delta_t} + \phi_g \sqrt{\Delta_t} G_t + \Sigma_g \frac{W_{t+\Delta_t}^g}{\sqrt{\Delta_t}}. \end{aligned} \quad (21)$$

If the latent factors were observable without error, Equation (21) could be estimated directly using ordinary least squares; in this case, the moment conditions are

$$\begin{aligned} E \{ W_{t+\Delta_t}^x \} &= \vec{0} & E \{ W_{t+\Delta_t}^g \} &= 0 \\ E \{ W_{t+\Delta_t}^x X_t' \} &= \vec{0} & E \{ W_{t+\Delta_t}^g G_t \} &= 0 \\ E \{ W_{t+\Delta_t}^x W_{t+\Delta_t}^{x'} \} &= \Sigma_x \Sigma_x' & E \left\{ \left(W_{t+\Delta_t}^g \right)^2 \right\} &= \Sigma_g^2. \end{aligned} \quad (22)$$

However, because the latent factors are estimated with error (equation 18), the empirical analog of Equation (22) cannot be implemented directly. Instead, we have that

$$\begin{aligned} \hat{W}_{t+\Delta_t}^x &= \frac{\hat{Y}_{t+\Delta_t}}{\sqrt{\Delta_t}} - \sqrt{\Delta_t} \left(\mu_x + \phi_x \hat{X}_t \right) \\ &= W_{t+\Delta_t}^x + \frac{\nu_{t+\Delta_t}^x - \nu_t^x}{\sqrt{\Delta_t}} - \sqrt{\Delta_t} \phi_x \nu_t^x \\ \hat{W}_{t+\Delta_t}^x \hat{X}_t' &= \left(W_{t+\Delta_t}^x + \frac{\nu_{t+\Delta_t}^x - \nu_t^x}{\sqrt{\Delta_t}} - \sqrt{\Delta_t} \phi_x \nu_t^x \right) (X_t + \nu_t^x)' \\ \hat{W}_{t+\Delta_t}^x \hat{W}_{t+\Delta_t}^{x'} &= \left(W_{t+\Delta_t}^x + \frac{\nu_{t+\Delta_t}^x - \nu_t^x}{\sqrt{\Delta_t}} - \sqrt{\Delta_t} \phi_x \nu_t^x \right) \left(W_{t+\Delta_t}^x + \frac{\nu_{t+\Delta_t}^x - \nu_t^x}{\sqrt{\Delta_t}} - \sqrt{\Delta_t} \phi_x \nu_t^x \right)', \end{aligned} \quad (23)$$

for the conventional factors X_t , and a parallel equation for the green factor G_t . Taking expectations of Equation (23), armed with the variance of ν_t^x , Ξ_t^x , and its covariance with $\nu_{t+\Delta_t}^x$ (the calculation of both of which we describe in further detail below), leads to the

usable moment conditions

$$\begin{aligned}
E \left\{ \hat{W}_{t+\Delta_t}^x \right\} &= \vec{0} \\
E \left\{ \hat{W}_{t+\Delta_t}^x \hat{X}_t' \right\} &= \frac{\text{COV} \left\{ \nu_{t+\Delta_t}^x, \nu_t^x \right\}}{\sqrt{\Delta_t}} - \underbrace{\left(\frac{I}{\sqrt{\Delta_t}} + \sqrt{\Delta_t} \phi_x \right)}_{\equiv \Phi_t^x} \Xi_t^x \\
E \left\{ \hat{W}_{t+\Delta_t}^x \hat{W}_{t+\Delta_t}^{x'} \right\} &= \Sigma_x \Sigma_x' + \frac{\Xi_{t+1}^x}{\Delta_t} + \Phi_t^x \Xi_t^x \Phi_t^{x'} - \frac{\text{COV} \left\{ \nu_{t+\Delta_t}^x, \nu_t^x \right\}}{\sqrt{\Delta_t}} \Phi_t^{x'} - \Phi_t^x \frac{\text{COV} \left\{ \nu_{t+\Delta_t}^x, \nu_t^x \right\}}{\sqrt{\Delta_t}},
\end{aligned}$$

where the second line defines the matrix Φ_t^x , and a similar equation holds for the green factor G_t . Define

$$\begin{aligned}
q_t^x &\equiv \begin{bmatrix} \hat{W}_{t+\Delta_t}^x \\ \text{vec} \left\{ \hat{W}_{t+\Delta_t}^x \hat{X}_t' - \frac{\text{COV} \left\{ \nu_{t+\Delta_t}^x, \nu_t^x \right\}}{\sqrt{\Delta_t}} + \Phi_t^x \Xi_t^x \right\} \\ \text{vech} \left\{ \hat{W}_{t+\Delta_t}^x \hat{W}_{t+\Delta_t}^{x'} - \Sigma_x \Sigma_x' - \frac{\Xi_{t+1}^x}{\Delta_t} - \Phi_t^x \Xi_t^x \Phi_t^{x'} \right. \\ \left. + \frac{\text{COV} \left\{ \nu_{t+\Delta_t}^x, \nu_t^x \right\}}{\sqrt{\Delta_t}} \Phi_t^{x'} + \Phi_t^x \frac{\text{COV} \left\{ \nu_{t+\Delta_t}^x, \nu_t^x \right\}}{\sqrt{\Delta_t}} \right\} \end{bmatrix} \\
q_t^g &\equiv \begin{bmatrix} \hat{W}_{t+\Delta_t}^g \\ \hat{W}_{t+\Delta_t}^g \hat{G}_t' - \frac{\text{COV} \left\{ \nu_{t+\Delta_t}^g, \nu_t^g \right\}}{\sqrt{\Delta_t}} + \Phi_t^g \Xi_t^g \\ \left(\hat{W}_{t+\Delta_t}^g \right)^2 - \Sigma_g^2 - \frac{\Xi_{t+1}^g}{\Delta_t} - \left(\Phi_t^g \right)^2 \Xi_t^g + 2 \frac{\text{COV} \left\{ \nu_{t+\Delta_t}^g, \nu_t^g \right\}}{\sqrt{\Delta_t}} \Phi_t^g \end{bmatrix}. \tag{24}
\end{aligned}$$

Then, our time series estimates of the parameters in equations (2) and (3) are those that set $\sum_t q_t^x = \sum_t q_t^g = 0$ in sample.

To compute the standard errors of the time-series parameters, we must compute the variance matrices of the measurement errors Ξ_t^x and Ξ_t^g , as well as the covariances of the measurement errors over time. To do so, we follow [Andreasen and Christensen \(2015\)](#) and account for the latency of the factors X_t from two sources: (1) sampling variation at t , and

(2) sampling variation in θ^* itself (and through it, the factor loadings). We compute

$$\Xi_t = \frac{1}{n_t} A_t^{-1} V_t A_t^{-1},$$

where

$$A_t = \frac{1}{n_t} J_t' J_t$$

$$J_t = \frac{\partial \hat{P}_{it}}{\partial X_t}$$

and

$$V_t = B_t + \sqrt{\frac{n_t}{N}} C_t \left(A^{\theta^*} \right)^{-1} \left(\sqrt{\frac{n_t}{N}} B^{\theta^*} \left(A^{\theta^*} \right)^{-1} - 2 \hat{\Sigma}_t^M \right) C_t'$$

$$B_t = \hat{\Sigma}_t^M A_t$$

$$C_t = \frac{1}{n_t} J_t' \mathcal{X}_t,$$

and then define Ξ_t^x as the upper-left 4×4 block of Ξ_t , and Ξ_t^g as the lower-right element of Ξ_t . Note that the latter is undefined in the early sample before green bonds are issued; for these values of t , Ξ_t is a 4×4 matrix. Likewise, in the early sample the J_t matrices are the second through fifth columns of the measurement matrix in equation (13); in the later sample including green bonds, the J_t matrices are the second through sixth columns of the measurement matrix.

Finally, to compute $\text{cov} \{ \nu_{t+\Delta_t}^x, \nu_t^x \}$ and $\text{cov} \{ \nu_{t+\Delta_t}^g, \nu_t^g \}$, we estimate a daily AR(1) on the realized bond-level residuals:

$$\frac{\eta_{i,t+\Delta_t}}{\sqrt{\Delta_t}} = \rho \eta_{i,t} \sqrt{\Delta_t} + \frac{\varepsilon_{i,t+\Delta_t}^m}{\sqrt{\Delta_t}},$$

where the variance of $\varepsilon_{i,t+\Delta_t}^m$ is $\Delta_t \sigma_m^2$ and the $\sqrt{\Delta_t}$ terms correct for the varying number of

days between observations in the sample. On each date, we use the estimated values of ρ and σ_m^2 to construct the $n_{t+\Delta_t} \times n_t$ matrix of bond-level measurement error autocovariances $\Sigma_{t+\Delta_t,t}$, with (i, j) element given by

$$(\Sigma_{t+\Delta_t,t})_{ij} \equiv \begin{cases} \rho^{\Delta_t} \frac{\sigma_m^2}{1-\rho^2} & \text{if bond } i \text{ at } t + \Delta_t \text{ is the same CUSIP as bond } j \text{ at } t \\ 0 & \text{otherwise} \end{cases}$$

We then construct

$$\text{c}\hat{\text{ov}} \{\nu_{t+\Delta_t}, \nu_t\} = \frac{1}{n_{t+\Delta_t}} \frac{1}{n_t} A_{t+\Delta_t}^{-1} J'_{t+\Delta_t} \Sigma_{t+\Delta_t,t} J_t A_t^{-1}$$

and define $\text{c}\hat{\text{ov}} \{\nu_{t+\Delta_t}^x, \nu_t^x\}$ as the upper 4×4 block of $\text{c}\hat{\text{ov}} \{\nu_{t+\Delta_t}, \nu_t\}$, while $\text{c}\hat{\text{ov}} \{\nu_{t+\Delta_t}^g, \nu_t^g\}$ is the lower-right element of the same matrix.

Finally, we estimate the standard errors of the time-series parameters $\{\mu_i, \phi_i, \Sigma_i \Sigma_i'\}$ where $i \in \{x, g\}$, as the usual GMM standard errors, accounting for Ξ_t^i :

$$\text{asymVar}(\theta_i) = \frac{1}{T_i} (R_i S_i^{-1} R_i')^{-1},$$

where

$$S_i \equiv \frac{1}{T_i - 1} \sum_{t=1}^{T_i} q_t^i q_t^{i'}$$

$$R_i \equiv \frac{1}{T_i - 1} \sum_{t=1}^{T_i} \frac{\partial q_t^i}{\partial \theta_i}$$

and q_t^i is defined in Equation (24). Notice that this procedure accounts for the different number of time-series observations in the green and conventional samples.

D Factor Loadings

In this section we plot a collection of factor loadings implied by our estimates. Figure 12 plots the conventional yield implied by our model estimates; specifically, the figure plots the four loadings $B^y(\tau)$ from

$$Y(\tau) = \hat{A}(\tau) + \hat{B}(\tau)' X_t \quad (25)$$

where $Y(\tau) \equiv -\frac{1}{\tau} \log P_t(\tau)$. We denote these loadings as \hat{A} and \hat{B} to distinguish them from the price loadings given by equation (8). Differently from the standard exponential-affine models, these loadings represent the first derivative of the log yield at maturity τ , which is given by

$$\hat{B}(\tau, X) \equiv \frac{\partial}{\partial X} \left\{ -\frac{1}{\tau} \log P_t(\tau) \right\} = \frac{-B(\tau)}{\tau [A(\tau) + B(\tau)' X]}.$$

The loadings in Figure 12 are evaluated at the sample average of the factors X_t and show that the 4 factors preserve the usual interpretation of level, slope, and two curvature factors. Figure 13 plots the loadings on the model-implied greenium, which are given by

$$Y_t^g(\tau) - Y_t(\tau) = \hat{A}^g(\tau) + \hat{B}^g(\tau)' X_t + \hat{C}^g(\tau) G_t. \quad (26)$$

Notice that the greenium loads mostly on the green factor G_t , as it should, but also to a small extent on the conventional factors X_t , primarily at the short end of the yield curve. This means that shorter-term green bonds load on the conventional factors differently from the conventional bonds of the same maturity, such that, in the spread between green and conventional yields, the loadings on average do not offset each other completely. This implies that short-term green and conventional bonds react differently to shifts in the stance of monetary policy and duration risk.

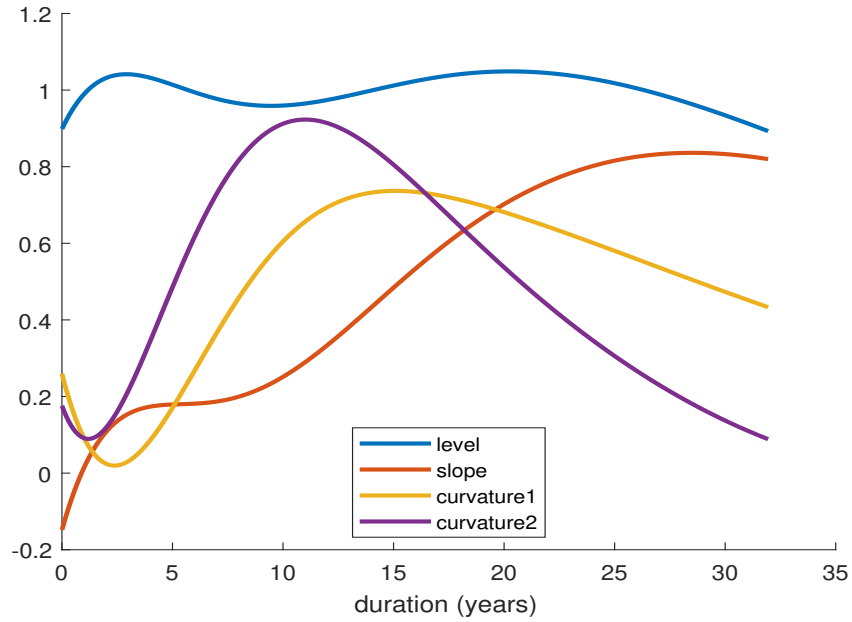


Figure 12. Yield Factor Loadings

The figure plots the conventional yield factor loadings $\hat{B}(\tau)$ from equation (25) as a function of maturity τ , evaluated at the average value of the factors.

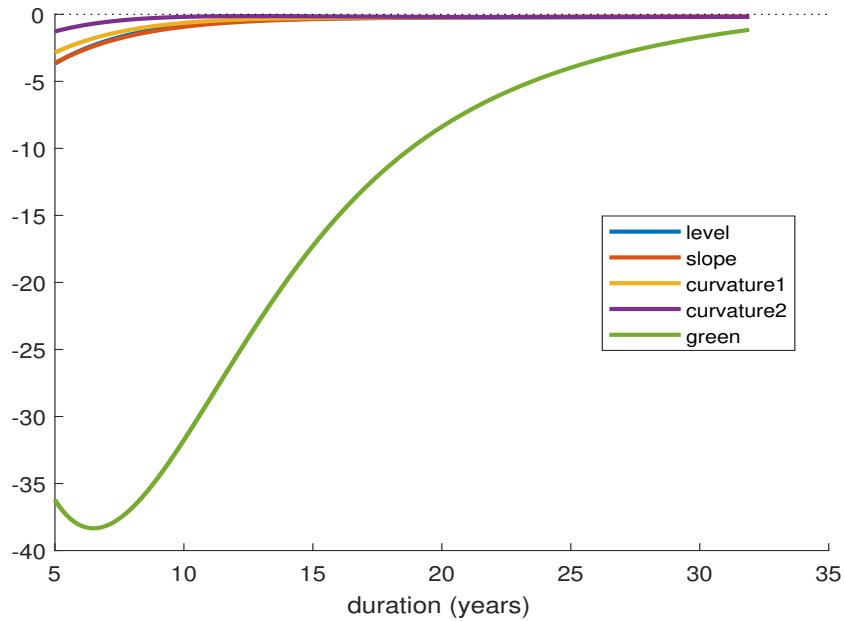


Figure 13. Greenium Factor Loadings

The figure plots the greenium loadings $\hat{B}^g(\tau)$ and $\hat{C}^g(\tau)$ from equation (26) as a function of maturity τ , evaluated at the average value of the factors.

Figure 13 plots the model-implied yield loadings of the greenium, defined as the model-implied yield difference between a τ -maturity zero-coupon green bond and a τ -maturity conventional bond, to the green factor G_t . The figure shows that although the greenium loads most strongly on G_t , as expected, the greenium also depends to a small extent on the conventional factors X_t , primarily at the short end of the yield curve. This means that shorter-term green bonds load on the conventional factors differently from the conventional bonds of the same maturity, such that, in the spread between green and conventional yields, the loadings on average do not offset each other completely. This implies that short-term green and conventional bonds react differently to shifts in the stance of monetary policy and duration risk.

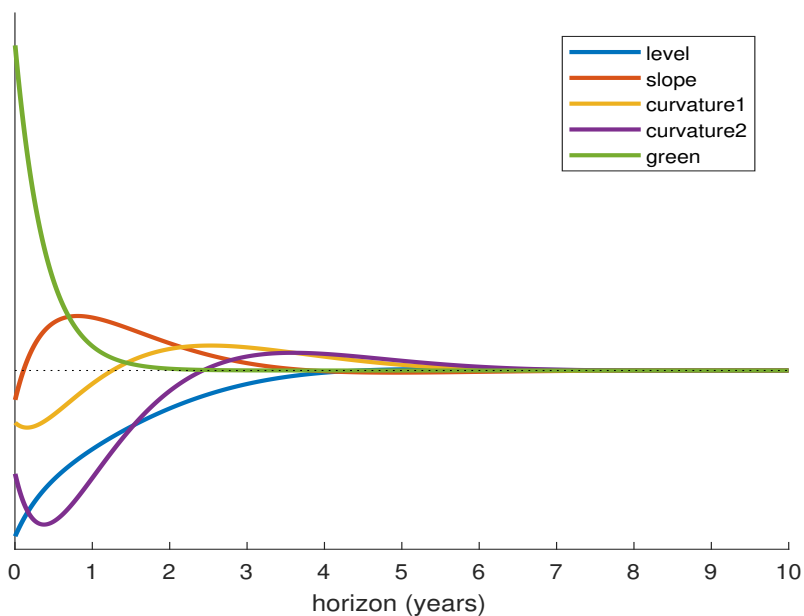


Figure 14. Forecast Loadings

The figure panel plots the greenium forecast loadings $B_\tau^f(h)$ and $C_\tau^f(h)$ from equation (28), where τ is fixed at 10 years and the x axis plots the loadings as a function of horizon h .

To derive short-horizon expected green excess returns, consider forecasting the price spread between two maturity-matched green and conventional bonds h periods into the future. Denote the future green-conventional price difference at maturity τ , for holding

period h , as

$$\Delta P_{t+h}(\tau - h) \equiv P_{t+h}^g(\tau - h) - P_{t+h}(\tau - h). \quad (27)$$

For a given τ , by iterating equations (2) and (3) forward in time, the expected value of equation (27) at time t , for various horizons h , depends only on the factors X_t and G_t .

Denote these forecast loadings as

$$E_t \Delta P_{t+h}(\tau - h) = A_\tau^f(h) + B_\tau^f(h)' X_t + C_\tau^f(h) G_t. \quad (28)$$

Figure 14 plots the $B_\tau^f(h)$ and $C_\tau^f(h)$ loadings as a function of h . As h approaches maturity (in this case 10 years), all loadings converge to zero, since the green and conventional bonds pay the same \$1 at maturity. However, over short horizons, forecasts depend not only on G_t , but also on the four conventional factors. In particular, when G_t is low, the conventional X_t factors play a larger role, and it is possible for the price spread ΔP_{t+h} to be expected to widen over a short horizon, inducing a positive expected green excess return.

Figure 14 shows that the G_t loading of the green-conventional price difference is positive, meaning that when 10-year green bonds are trading at a premium to conventional bonds (implying a lower yield, see Figure 13), then they are expected to continue to trade at a premium for just a few years on average. However, because 10-year bonds are quite sensitive to interest rate risk, high interest rates (e.g. a high level factor, plotted in blue in Figure 14) mitigate this effect. The second curvature factor (plotted in purple), which loads primarily on 8–10 year bonds, has a similar effect. In fact, because the level and curvature loadings are so much flatter than the G_t loading, when (for example) the level factor is high enough it is possible for green bonds to be trading at a premium to conventional bonds today, to trade at a discount in the medium term, and then to trade very close to conventional bonds over long horizons. In other words, while the greenium captures the price differential (expressed as an interest rate) at t , expected green excess returns at $t + h$ can vary widely depending on the

current conventional factors, especially for horizons that are much shorter than maturity.

References

- Alekseev, Georgij, Stefano Giglio, Quinn Maingi, Julia Selgrad, and Johannes Stroebel.** 2021. “A quantity-based approach to constructing climate risk hedge portfolios.” Working Paper. 7
- Andreasen, Martin M., and Bent Jesper Christensen.** 2015. “The SR approach: A new estimation procedure for non-linear and non-gaussian dynamic term structure models.” *Journal of Econometrics*, 184(2): 420–451. 20, 49, 54
- Andreasen, Martin M., Jens H.E. Christensen, and Glenn D. Rudebusch.** 2019. “Term structure analysis with Big Data: One-step estimation using bond prices.” *Journal of Econometrics*, 212(1): 26–46. 12
- Ardia, David, Keven Bluteau, Kris Boudt, and Koen Inghelbrecht.** 2022. “Climate change concerns and the performance of green vs. brown stocks.” *Management Science*. 35
- Baker, Malcolm, Daniel Bergstresser, George Serafeim, and Jeffrey Wurgler.** 2018. “Financing the response to climate change: The pricing and ownership of U.S. green bonds.” National Bureau of Economic Research Working Paper 25194. 6
- Bansal, Ravi, Dana Kiku, and Marcelo Ochoa.** 2016. “Price of long-run temperature shifts in capital markets.” National Bureau of Economic Research. 7
- Bauer, Michael D, and Glenn D Rudebusch.** 2021. “The rising cost of climate change: Evidence from the bond market.” *The Review of Economics and Statistics*, 1–45. 7
- Bauer, Rob, Tobias Ruof, and Paul Smeets.** 2021. “Get real! Individuals prefer more sustainable investments.” *The Review of Financial Studies*, 34(8): 3976–4043. 7
- Berardi, Andrea, Roger Brown, and Stephen M Schaefer.** 2021. “Bond risk premia: The information in (really) long term rates.” Working Paper. 21

- Berg, Florian, Julian F Kölbel, and Roberto Rigobon.** 2022. “Aggregate confusion: The divergence of ESG ratings.” *Review of Finance*, 26(6): 1315–1344. 6
- Berg, Florian, Julian F Kölbel, Anna Pavlova, and Roberto Rigobon.** 2021. “ESG confusion and stock returns: Tackling the problem of noise.” *Working Paper*. 6
- Bernstein, Asaf, Matthew T Gustafson, and Ryan Lewis.** 2019. “Disaster on the horizon: The price effect of sea level rise.” *Journal of Financial Economics*, 134(2): 253–272. 7
- Berrada, Tony, Leonie Engelhardt, Rajna Gibson, and Philipp Krueger.** 2022. “The economics of sustainability linked bonds.” *Swiss Finance Institute Research Paper*, , (22-26). 7
- Bolton, Patrick, and Marcin Kacperczyk.** 2021. “Do investors care about carbon risk?” *Journal of Financial Economics*, 142(2): 517–549. 7
- Bonnefon, Jean-François, Augustin Landier, Parinitha R Sastry, and David Thesmar.** 2022. “The moral preferences of investors: Experimental evidence.” National Bureau of Economic Research. 7
- Caramichael, John, and Andreas C Rapp.** 2022. “The green corporate bond issuance premium.” *International Finance Discussion Paper*, , (1346). 6
- Cevik, Serhan, and João Tovar Jalles.** 2022. “An apocalypse foretold: Climate shocks and sovereign defaults.” *Open Economies Review*, 33(1): 89–108. 7
- Chikhani, Pauline, and Jean-Paul Renne.** 2022. “Climate linkers: Rationale and pricing.” *Available at SSRN 3881262*. 7
- Cochrane, John H., and Monika Piazzesi.** 2008. “Decomposing the yield curve.” *Working paper*. 21

- Colombage, Sisira, and KGM Nanayakkara.** 2020. “Impact of credit quality on credit spread of Green Bonds: a global evidence.” *Review of Development Finance*, 10(1): 31–42. 6
- D’Amico, Stefania, and N Aaron Pancost.** 2021. “Special repo rates and the cross-section of bond prices: The role of the special collateral risk premium.” *Review of Finance*, 26(1): 117–162. 15, 16
- D’Amico, Stefania, Don H. Kim, and Min Wei.** 2018. “Tips from TIPS: The informational content of treasury inflation-protected security prices.” *Journal of Financial and Quantitative Analysis*, 53(1): 395–436. 9
- Deutsche Finanzagentur.** 2022. “Federal Republic of Germany Green Bond Investor Presentation.” *Presentation slides*. 47
- Duffie, Darrell.** 1996. “Special repo rates.” *The Journal of Finance*, 51(2): 493–526. 15
- Edmans, Alex, Doron Levit, and Jan Schneemeier.** 2022. “Socially responsible divestment.” *European Corporate Governance Institute–Finance Working Paper*, , (823). 6
- Engle, Robert F, Stefano Giglio, Bryan Kelly, Heebum Lee, and Johannes Stroebel.** 2020. “Hedging climate change news.” *The Review of Financial Studies*, 33(3): 1184–1216. 7
- Flammer, Caroline.** 2021. “Corporate green bonds.” *Journal of Financial Economics*, 142(2): 499–516. 6
- Fontaine, Jean-Sébastien, and René Garcia.** 2012. “Bond Liquidity Premia.” *Review of Financial Studies*, 25(4): 1207–1254. 8
- Gabaix, Xavier.** 2007. “Linearity-generating processes: A modelling tool yielding closed forms for asset prices.” National Bureau of Economic Research Working Paper 13430. 15

- Gabaix, Xavier.** 2008. “Variable rare disasters: A tractable theory of ten puzzles in macro-finance.” *The American Economic Review*, 98(2): 64–67. 15
- Gibson, Rajna, Philipp Krueger, and Shema F Mitali.** 2020. “The sustainability footprint of institutional investors: ESG driven price pressure and performance.” *Swiss Finance Institute Research Paper*, , (17-05). 7
- Giglio, Stefano, Matteo Maggiori, Krishna Rao, Johannes Stroebe, and Andreas Weber.** 2021. “Climate change and long-run discount rates: Evidence from real estate.” *The Review of Financial Studies*, 34(8): 3527–3571. 7
- Guenster, Nadja, Daniel Brodback, Sébastien Pouget, and Ruichen Wang.** 2022. “The Valuation of Corporate Social Responsibility: A Willingness to Pay Experiment.” Available at SSRN 4260824. 7
- Hansen, Lars Peter.** 2022. “Central banking challenges posed by uncertain climate change and natural disasters.” *Journal of Monetary Economics*, 125: 1–15. 6
- Hartzmark, Samuel M, and Abigail B Sussman.** 2019. “Do investors value sustainability? A natural experiment examining ranking and fund flows.” *The Journal of Finance*, 74(6): 2789–2837. 7
- Hartzmark, Samuel M, and Kelly Shue.** 2023. “Counterproductive sustainable investing: The impact elasticity of brown and green firms.” Working Paper, Boston College. 6
- Heeb, Florian, Julian F Kölbel, Falko Paetzold, and Stefan Zeisberger.** 2023. “Do investors care about impact?” *The Review of Financial Studies*, 36(5): 1737–1787. 7, 43
- Huynh, Thanh D, and Ying Xia.** 2021. “Climate change news risk and corporate bond returns.” *Journal of Financial and Quantitative Analysis*, 56(6): 1985–2009. 7

- Ilhan, Emirhan, Zacharias Sautner, and Grigory Vilkov.** 2021. “Carbon tail risk.” *The Review of Financial Studies*, 34(3): 1540–1571. 7
- Kapraun, Julia, Carmelo Latino, Christopher Scheins, and Christian Schlag.** 2021. “(In)-credibly green: Which bonds trade at a green bond premium?” 6
- Karpf, Andreas, and Antoine Mandel.** 2018. “The changing value of the greenlabel on the US municipal bond market.” *Nature Climate Change*, 8(2): 161–165. 6
- Kling, Matthew M, Stephanie L Auer, Patrick J Comer, David D Ackerly, and Healy Hamilton.** 2020. “Multiple axes of ecological vulnerability to climate change.” *Global Change Biology*, 26(5): 2798–2813. 7
- Kölbel, Julian F, and Adrien-Paul Lambillon.** 2022. “Who pays for sustainability? An analysis of sustainability-linked bonds.” *An Analysis of Sustainability-Linked Bonds (January 12, 2022). Swiss Finance Institute Research Paper*, , (23-07). 7
- Krishnamurthy, Arvind.** 2002. “The Bond/Old-Bond Spread.” *Journal of Financial Economics*, 66(2–3): 463–506. 8
- Krueger, Philipp, Zacharias Sautner, and Laura T Starks.** 2020. “The importance of climate risks for institutional investors.” *The Review of Financial Studies*, 33(3): 1067–1111. 7
- Larcker, David F., and Edward M. Watts.** 2020. “Where’s the greenium?” *Journal of Accounting and Economics*, 69(2): 0–101312. 6
- Le, Anh, and Kenneth J Singleton.** 2013. “The structure of risks in equilibrium affine models of bond yields.” *Working paper, University of North Carolina at Chapel Hill*. 21
- Litterman, Robert, and Jose Scheinkman.** 1991. “Common factors affecting bond returns.” *Journal of Fixed Income*, 1(1): 54–61. 21

- Loumioti, Maria, and George Serafeim.** 2022. “The issuance and design of sustainability-linked loans.” *Available at SSRN*. 7
- Painter, Marcus.** 2020. “An inconvenient cost: The effects of climate change on municipal bonds.” *Journal of Financial Economics*, 135(2): 468–482. 7
- Pancost, N. Aaron.** 2021. “Zero-coupon yields and the cross-section of bond prices.” *The Review of Asset Pricing Studies*, 11(2): 209–268. 8, 12, 19, 20, 32
- Papoutsis, Melina, Monika Piazzesi, and Martin Schneider.** 2021. “How unconventional is green monetary policy.” *JEEA-FBBVA Lecture at the ASSA (January)*. 6
- Pastor, Lubos, Robert F. Stambaugh, and Lucian A. Taylor.** 2021. “Sustainable investing in equilibrium.” *Journal of Financial Economics*, 142(2): 550–571. 5, 6, 16, 35, 42
- Pastor, Lubos, Robert F. Stambaugh, and Lucian A. Taylor.** 2022. “Dissecting green returns.” *Journal of Financial Economics*, 146(2): 403–424. 5, 6, 42
- Pedersen, Lasse Heje, Shaun Fitzgibbons, and Lukasz Pomorski.** 2021. “Responsible investing: The ESG-efficient frontier.” *Journal of Financial Economics*, 142(2): 572–597. 7
- Pietsch, Allegra, and Dilyara Salakhova.** 2022. “Pricing of green bonds: Drivers and dynamics of the greenium.” 44
- Riedl, Arno, and Paul Smeets.** 2017. “Why do investors hold socially responsible mutual funds?” *The Journal of Finance*, 72(6): 2505–2550. 7
- Riedler, Jesper, and Tina Koziol.** 2021. “Scaling, unwinding and greening QE in a calibrated portfolio balance model.” *ZEW Discussion Papers*, 21. 6
- Sautner, Zacharias, Laurence Van Lent, Grigory Vilkov, and Ruishen Zhang.** 2023. “Firm-level climate change exposure.” *The Journal of Finance*, 78(3): 1449–1498. 7

- Semmler, Willi, Joao Paulo Braga, Andreas Lichtenberger, Marieme Toure, and Erin Hayde.** 2021. “Fiscal policies for a low-carbon economy.” 5
- Starks, Laura T.** 2023. “Presidential address: Sustainable finance and ESG issues—value versus values.” *The Journal of Finance*. 7
- Stroebel, Johannes, and Jeffrey Wurgler.** 2021. “What do you think about climate finance?” *Journal of Financial Economics*, 142(2): 487–498. 7
- Zerbib, Olivier David.** 2019. “The effect of pro-environmental preferences on bond prices: Evidence from green bonds.” *Journal of Banking & Finance*, 98: 39–60. 6, 7
- Zerbib, Olivier David.** 2022. “A sustainable capital asset pricing model (S-CAPM): Evidence from environmental integration and sin stock exclusion.” *Review of Finance*, 26(6): 1345–1388. 6